# Calming the Cytokine Storm - Splenic Ultrasound for Treating Inflammatory Disorders and Potentially COVID-19


**Authors**

Rachel S. Graham[1], Daniel P. Zachs[2], Victoria Cotero[3], Catherine D'Agostino[4], Despoina Ntiloudi[5], Claire R.W. Kaiser[2], John Graf[3], Kirk Wallace[3], Thomas R. Coleman[5], Jeffrey Ashe[3], John Pellerito[4], Kevin J. Tracey[5], Bryce Binstadt[6], Sangeeta S. Chavan[4], Stavros Zanos[4], Christopher Puleo[3], Erik Peterson[7¶], and Hubert H. Lim[1,2¶]

**Affiliations**

[1]Department of Otolaryngology - Head & Neck Surgery, University of Minnesota, Minneapolis, MN, 55455, USA.
[2]Department of Biomedical Engineering, University of Minnesota, Minneapolis, MN, 55455, USA.
[3]General Electric Research, 1 Research Circle, Niskayuna, NY, 12309, USA.
[4]Department of Radiology, North Shore University Hospital, 300 Community Drive, Manhasset, NY, 11030, USA.
[5]Feinstein Institutes for Medical Research, 350 Community Drive, Manhasset, NY, 11030 USA.
[6]Center for Immunology and Department of Pediatrics, University of Minnesota, Minneapolis 55455, MN, USA
[7]Department of Medicine, Division of Rheumatic and Autoimmune Diseases, University of Minnesota, 420 Delaware Street SE, MMC 108, Minneapolis, MN, 55455, USA
[¶]These authors equally contributed as senior authors



**Abstract**

Hyperinflammation and uncontrolled cytokine release, which can be seen in severe cases of COVID-19, require therapy to reduce the innate immune response without hindering necessary adaptive immune mechanisms. Here, we show results from the first in-human trials using non-invasive ultrasound stimulation of the spleen to reduce cytokine release in the context of both an acute response in healthy subjects and a chronic inflammatory condition in rheumatoid arthritis patients. Splenic ultrasound results in a reduction in TNF serum levels, as well as IL-1β and IL-8 transcript levels in monocytes. There is also a down regulation of pathways involved in TNF and IL-6 production, and IFNγ- and NFκB-regulated genes. Many of these cytokines or pathways are upregulated in COVID-19 patients. There is also a reduction in chemokine transcript levels and other components of the chemotactic response, suggesting that reduction of cellular migration may contribute to the therapeutic effects of ultrasound. There is no inhibition of the adaptive immune response with ultrasound treatment relating to antibody production. This is consistent with a pre-clinical animal model where enhanced antibody production was achieved with splenic ultrasound. Therefore, this new splenic ultrasound approach has the potential to treat acute and chronic hyper-inflammatory diseases, as it lowers cytokine levels without disrupting the normal adaptive immune response. Portable ultrasound technologies are currently being developed and translated to the clinic to treat various inflammatory disorders, with more recent efforts directed towards combatting the hyperinflammation or 'cytokine storm' in COVID-19 patients.

## Introduction

Cytokines release by cells of the innate immune system drive inflammation (*1, 2*). Inflammatory reactions are typical in response to microbial or viral infection but can lead to health problems or life-threatening conditions if there is a persistent hyperactive innate immune response, involving cytokine toxicity and tissue damage (*2, 3*). A recent and devastating example is the hyperinflammation caused by the coronavirus disease 2019 (COVID-19, disease associated with SARS-CoV-2 viral infection). It is estimated that 17% of COVID-19 cases experience a 'cytokine storm' that leads to severe or fatal respiratory disease, known as acute respiratory distress syndrome (ARDS) (*4-6*). In addition to other acute conditions, such as sepsis and acute kidney injury (*7, 8*), hyperinflammation is an issue that occurs across multiple chronic inflammatory systemic diseases, such as rheumatoid arthritis (RA) and irritable bowel syndrome (*9, 10*). The current pharmacologic approaches to treating hyperinflammation are associated with multiple side effects and high costs.

Over the past 20 years, researchers within the field of bioelectronic medicine have investigated an unconventional approach for treating inflammation through the use of vagus nerve stimulation (*11-13*). Electrical stimulation of the vagus nerve activates the splenic nerve and cells within the spleen, leading to activation of the cholinergic anti-inflammatory pathway (*14, 15*). This pathway depends on splenic nerve release of norepinephrine that activates acetyltransferase -expressing T lymphocytes, which in turn modulates innate immune cells to decrease systemic levels of key pro-inflammatory cytokines, such as IL-6, IL-15 and TNF (*16, 17*). Furthermore, electrical vagus nerve stimulation has been shown in mice and humans to provide therapeutic anti-inflammatory effects for chronic inflammatory diseases (e.g., RA and irritable bowel syndrome) and for acute inflammation (e.g., sepsis, renal ischemia, trauma/hemorrhagic shock, and acute lung injury following trauma/hemorrhagic shock; (*16, 18-21*).

Direct vagus nerve stimulation requires invasive implantation procedures. Several groups have pursued non-invasive ultrasound stimulation of the spleen as a safer, non-surgical approach for modulating the cholinergic anti-inflammatory pathway. Since the vagus nerve projects to the brain and multiple organs throughout the body (*22*), targeting neurons or cells specifically within the spleen can reduce unintended activation or side effects. There has been a recent surge of research which demonstrates the ability to activate or modulate cells with ultrasound energy (*23-28*) There are several studies in rodents showing the ability to modulate the splenic nerve or immune cells within the spleen with ultrasound, to reduce inflammation and cytokine levels (*29-33*). One of the initial reports was in a mouse model of reperfusion injury and kidney inflammation, where ultrasound stimulation of the spleen significantly reduced kidney damage (*29, 34*). Recently, our research groups discovered that specific parameters of ultrasound stimulation of the spleen can drive significant anti-inflammatory effects in rodent models of both chronic inflammation (inflammatory arthritis) and acute inflammation (sepsis) (*31, 32*), which was shown to be mediated through a similar cholinergic anti-inflammatory pathway accessed through vagus nerve stimulation. Ultrasound is a potentially impactful clinical solution to inflammation as it can be applied non-invasively to the body with a wearable device and with energy parameters already shown to be safe for the human body based on numerous ultrasound imaging applications (*35, 36*).

Here, we show the first in-human results of pro-inflammatory cytokine reduction with non-invasive ultrasound stimulation of the spleen. In healthy individuals, a single three-minute administration of splenic ultrasound stimulation significantly inhibits whole blood TNF production upon *ex vivo* exposure to endotoxin compared to sham controls. In RA patients, we observed that

daily splenic ultrasound stimulation results in reduction of blood-borne transcripts encoding for pro-inflammatory markers IL-1β, IL-8, and NFκB, as well as suppresses pathways involved in IL-6 and TNF production. Ultrasound also reduces pathways involved with monocyte migration, contributing to its anti-inflammatory effect. From a safety perspective, circulating immune cell composition does not change with ultrasound treatment, and ultrasound does not inhibit the adaptive immune response in humans. Our additional pre-clinical animal data further demonstrates that in addition to dampening cytokine output and circulating monocyte invasiveness, prophylactic ultrasound activation of the splenic neuroimmune pathway results in enhanced antibody response upon exposure to an inflammatory antigen. Thus, activation of the splenic neuroimmune pathway may provide a low risk therapeutic approach for a broad range of health conditions, due to its pleotropic nature and physiological role in suppressing specific cytokines involved in innate immunity while enhancing the transition to and maintenance of the adaptive immune response (*18, 37, 38*). Together, these data suggest great potential for splenic ultrasound as a low-risk clinical therapy for a range of acute or chronic inflammatory diseases without requiring surgery or intake of artificial substances with possible side effects.

Considering that many of the same pro-inflammatory molecules suppressed by ultrasound are implicated as molecular drivers in COVID-19 patients with severe disease, ultrasound also has potential as a non-invasive therapy to combat this pandemic. Drug based suppression of these cytokines for tissue protection comes with the risk of inhibiting viral clearance or increasing susceptibility to bacterial co-infections (*39, 40*). Non-invasive ultrasound activation of the splenic neuroimmune pathway may provide an alternative method to combat the cytokine storm without compromising the adaptive immune response in COVID-19 patients, ultimately reducing the high mortality and morbidity rates confronting this worldwide pandemic that currently has limited treatment options.

## Results

### *Non-invasive Splenic Ultrasound Reduces TNF in Humans*

To investigate how non-invasive ultrasound stimulation of the spleen affects cytokine levels directly in human subjects, healthy participants were recruited into a study designed to investigate effect of different ultrasound parameters and locations of stimulation in the spleen on various immune and metabolic responses during acute stimulation (feasibility study described at clinicaltrials.gov: NCT03548116). Due to the urgency of identifying potential treatment options for COVID-19 patients, data pertaining specifically to ultrasound stimulation of the hilum of the spleen with the most effective intensity parameter in the study (corresponding to one cohort from the study) are presented in this paper.

Participants received pulsed ultrasound stimulation of the spleen for three minutes (2.2 MHz, 1 Hz pulse repetition frequency, 290.4 mW/cm$^2$ $I_{SPTA}$) using the GE LOGIQ E9 ultrasound system with the C1-6 probe. An ultrasonographer first identified and targeted the hilum of the spleen, then delivered the pulsed ultrasound stimulus using a modified elastography software setting in the system. Sham stimulation control subjects underwent the same procedure as the stimulated group, including transducer placement and movement of the ultrasound probe to the proper splenic location trajectory, but with no ultrasound energy being transmitted to the spleen from the transducer. Since healthy subjects have low serum TNF levels, we revealed changes in inflammatory status using whole blood challenged with lipopolysaccharide (LPS) *ex vivo*. This *ex*

*vivo* cytokine production assay has been previously used to verify splenic neuroimmune activation using implanted vagus nerve stimulators and is a well-established method for non-invasively assessing activation of neuroimmune pathways (*18, 41-43*). A reduction in LPS-induced TNF production in blood sampled from ultrasound stimulated subjects was tested at multiple LPS concentrations (Fig. 1A) and significant reduction is observed when comparing the ultrasound stimulated group to the non-stimulated controls (Fig. 1B; p-value = 0.006 using Wilcoxon unpaired rank-sum test) at the optimal LPS concentration (1 ng/mL; Fig.1A). These data are consistent with earlier reports using implanted nerve stimulators or pharmaceutical activators of the splenic pathway (*18, 42*). They are also consistent with the magnitude of TNF reduction using similar ultrasound stimulation parameters in a previous study activating the neuroimmune pathway in a rodent model of endotoxemia (*31*). Further supporting the human results, we also demonstrated that splenic ultrasound stimulation in a rodent model achieves a reduction across a number of pro-inflammatory cytokines beyond TNF, including IL-6, IFNγ, IL-1β, IL-1α, and IL-12 in splenic lysates (Fig. S1), which is consistent with previous reports using implanted vagus nerve stimulators (*18, 44*).

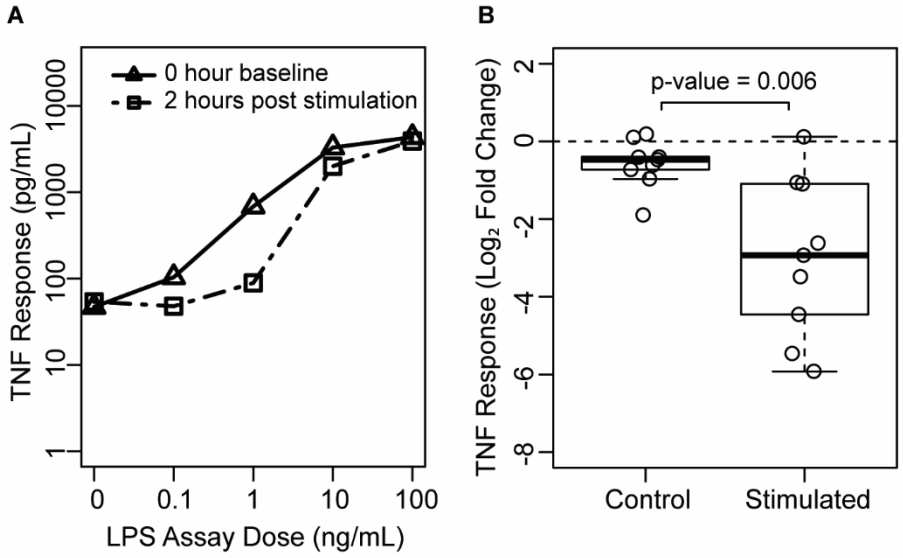


**Figure 1.** *Non-invasive ultrasound stimulation of the spleen reduces TNF production in human subjects*. A) Whole blood from all subjects and samples was incubated with LPS at multiple concentrations. TNF response after LPS incubation is shown for one ultrasound stimulated subject from samples collected before (0 hours baseline) and after (2 hours post stimulation) ultrasound application. The optimal dose of LPS for measuring the immunomodulatory response to ultrasound was found to be at 1 ng/mL, and this is used for comparing the TNF response between the ultrasound stimulated versus control groups. B) Ultrasound stimulation of the spleen decreases whole-blood LPS-induced TNF release, where blood was obtained from 18 healthy human subjects prior to and then two hours following splenic ultrasound application (stimulated: n=9, control: n=9). The data shown were taken from the 1 ng/ml LPS concentration for each dose response curve for all subjects and samples. p-value was computed using the unpaired Wilcoxon rank-sum test.

### *Pro-inflammatory Cytokines and Signaling Pathways are Downregulated in Circulating Monocytes with Ultrasound Treatment*

Previous animal research demonstrated that ultrasound can significantly reduce inflammation and improve clinical measures in a chronic inflammatory arthritis model (*32*). Expanding upon the findings in healthy human subjects in the previous section, we initiated a controlled, randomized clinical trial of splenic ultrasound treatment in RA patients (clinical study described at clinicaltrials.gov: NCT03690466). Participants received ultrasound stimulation to the spleen with the goal of lowering the over-active inflammatory response that occurs during RA flare-ups. Up to 20 RA patients are to be recruited into the study (enrollment is ongoing). Due to the urgency of

identifying treatment options for this COVID-19 pandemic, data from single-cell RNA sequencing (scRNA-seq) in peripheral blood mononuclear cells (PBMCs) that has been collected thus far in five ultrasound-treated patients have been analyzed ahead of completion of the study for inclusion into this paper. PBMCs were isolated from whole blood taken from each research participant before ultrasound treatment (day 0, pre-stimulation) and after two weeks of daily 30-minute sessions of ultrasound to the spleen (day 14, post-stimulation). From these 10 samples (subjects = 5, timepoints = 2), a total of 53,343 PBMCs were successfully sequenced from single cells (Table S1). *In silico* analysis identified 13 cell-types based on gene expression patterns of standardly used marker genes (Fig. S2). Participants received stimulation with a 1 MHz transducer (1.2 $W/cm^2$; SoundCare Plus, Roscoe Medical) that was moved continuously across a 5-inch by 5-inch square, centered on the spleen, as identified by an ultrasonographer. Further details on the clinical study design is presented in the *Materials and Methods* section.

We aimed to identify molecular changes that occur with splenic ultrasound in humans to better understand how this ultrasound treatment can drive an anti-inflammatory response. We observed reduced monocyte expression of key pro-inflammatory cytokine genes encoding for IL-1β and IL-8 from all five subjects post-stimulation compared with pre-stimulation (Fig. 2A, p-values given for transcripts showing significance of $p<0.05$). Although this result was determined by analyzing all monocytes, reduction of these two markers appears primarily in CD14+ monocytes as this is the cell type showing predominant expression of those genes (Fig. 2B). The same analysis in CD8+ T cells show a decrease in transcripts that encode for IFNγ (Fig. 2A). The changes in transcript level of these cytokines can only be detected when comparing within the same cell type before and after treatment, within the cell that expresses the cytokine (Fig. S2). Consistent with known expression patterns of *IL1B* and *CXCL8* transcripts (encoding for IL-1β and IL-8), we see that these transcripts are only suppressed in the monocytes where they are primarily detected. Likewise, *IFNG* transcripts (encoding for IFNγ) are detected and found to be reduced in CD8+ T cells (Fig. S2). In our dataset, other cytokines like TNF and IL-6 did not show a significant change in monocytes; however, IL-6 transcripts were detected in only 66 of the 53,343 cells. Therefore, we cannot definitively conclude if there is or is not a change in transcript levels encoding IL-6 with ultrasound treatment.

Since monocytes play a critical role in the innate immune system and the inflammatory response, we further focused our analyses on transcriptional changes that occur in circulating monocytes after ultrasound treatment. Differential expression analysis of all monocytes across the five subjects, pre- and post-ultrasound stimulation, shows 938 differentially expressed genes (p-value$<0.05$) with 841 of those genes being down-regulated. These results reveal an overall shift in reduction of gene transcripts in monocytes with ultrasound treatment. Additionally, this reduction in transcript levels did not appear as a result of sequencing differences, as we observe no obvious difference in the number of cells sequenced, the number of sequencing reads, or number of average genes detected per cell between monocytes taken from day 0 as compared to day 14 (Table S1, ‘CD14 Mono’ and ‘CD16 Mono’). Although these gene transcripts are defined as differentially expressed when comparing monocytes from all subjects (Fig. 2A), we also observe that for most genes, this down-regulation is consistent across subjects (Fig. 2C; columns represent cell-type averages for CD14+ and CD16+ cells for each subject that are similar across columns for many of the genes).

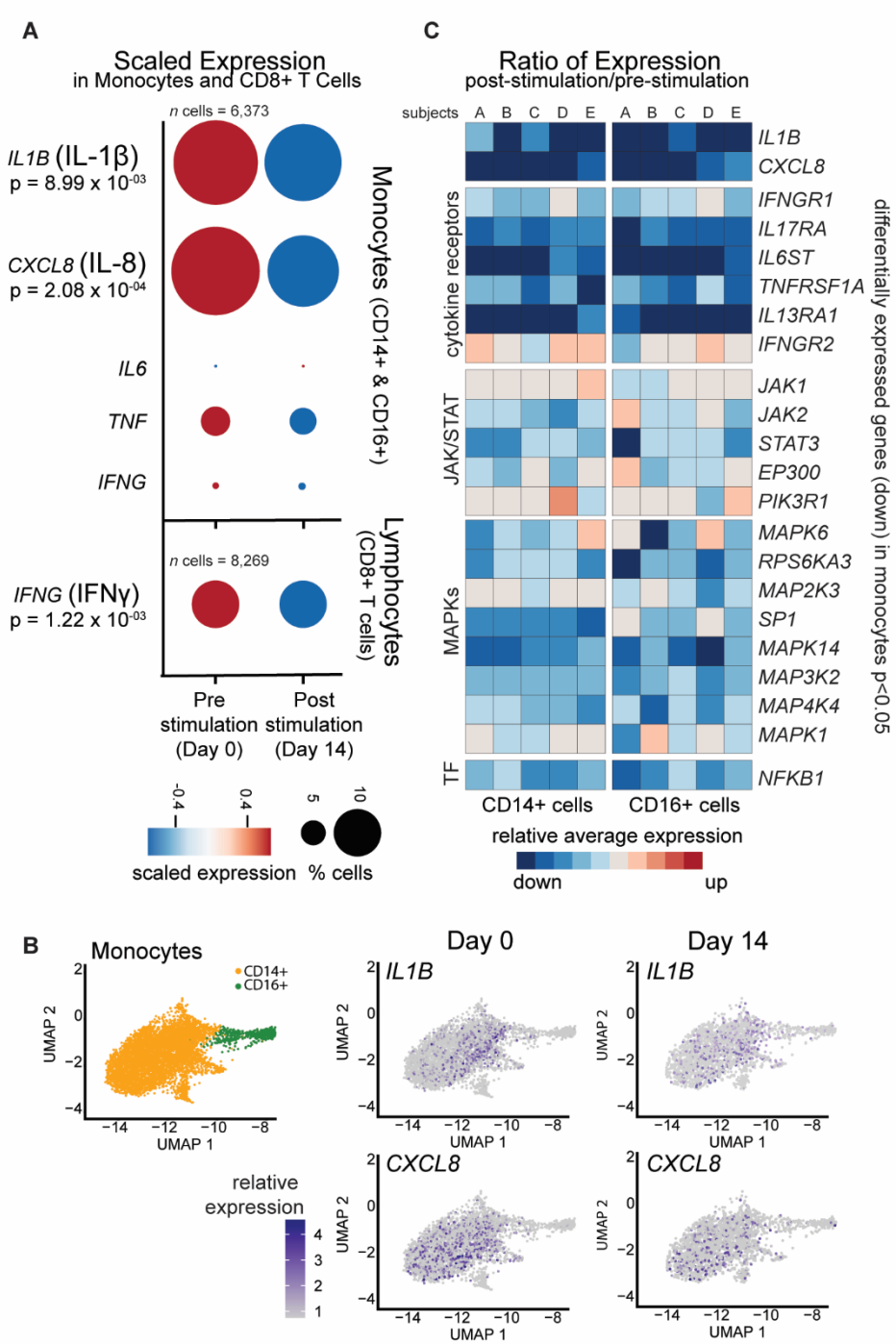


**Figure 2.** *Splenic ultrasound treatment reduces cytokines and downstream pathways in-vivo in RA patients.* A) Single cell RNA sequencing of PBMCs from RA patient receiving 14 days of 30-minute daily ultrasound stimulation of the spleen. Samples were collected pre- (day 0) and post-stimulation (day 14) with ultrasound. Dot plot shows percent of CD14+ and CD16+ monocytes (top) or CD8+ T cells (bottom) that express the transcript (labeled on the left) represented by size, and scaled expression level represented by color (obtained by subtracting the mean and dividing by the standard deviation). Key pro-inflammatory cytokines are shown with unadjusted p-values labeled for those transcripts significantly downregulated (p-value <0.05). B) UMAP showing top two dimensions (principal components) contributing to variability within the dataset. UMAP diagrams showing CD14+ and CD16+ monocytes represented by orange and green dots, respectively. IL-1β and CXCL8 expression on day 0 and day 14 are also mapped on these UMAP diagrams. C) Heatmap displaying the average relative expression (for all cells in specified group) of downregulated transcripts (genes listed on the right, p-value <0.05). Color denotes relative expression for post-ultrasound levels compared to (divided by) pre-ultrasound levels for each subject (represented by columns, n = 5, participant A-E shown left to right) in CD14+ cells or CD16+ cells. Genes encoding for cytokine receptors, components of the JAK/STAT pathway, MAP kinases, and transcription factor (TF) are grouped and labeled on the left of the plot.

These results are quite consistent given the high variability or inhomogeneity in age, sex, physical characteristics, disease properties and past treatments across subjects (participants A-E in Table S2 correspond to columns 1-5 in Fig. 2C, respectively). Within these down-regulated genes in monocytes, we also observe that many cytokine receptors, such as those for TNF, IL-6, IL-17, IL-13, and IFNγ were reduced with ultrasound treatment (Fig. 2C). Furthermore, components of signaling pathways downstream of these cytokines are also down regulated, including components of the JAK/STAT pathway, MAP kinases, and pro-inflammatory transcription factor NFκB (Fig. 2C). Together, these findings demonstrate a consistent and robust reduction in transcripts encoding key pro-inflammatory cytokines and cellular signaling molecules downstream of their receptors after 14 days of daily splenic ultrasound treatment across all five subjects.

*Suppression of Multiple Pathways that Contribute to the Pro-inflammatory Response*

Cytokines trigger multiple cellular pathways, which then contribute to systemic inflammation. Our transcriptomic data reveal that many genes known to be regulated by IFNγ and NFκB are subsequently downregulated with ultrasound treatment, further promoting a cascade of suppression across multiple pro-inflammatory pathways with ultrasound treatment (Fig. 3A). We sought to determine if the 840 down-regulated genes in monocytes showed statistical enrichment for functional Gene Ontology (GO)terms associated

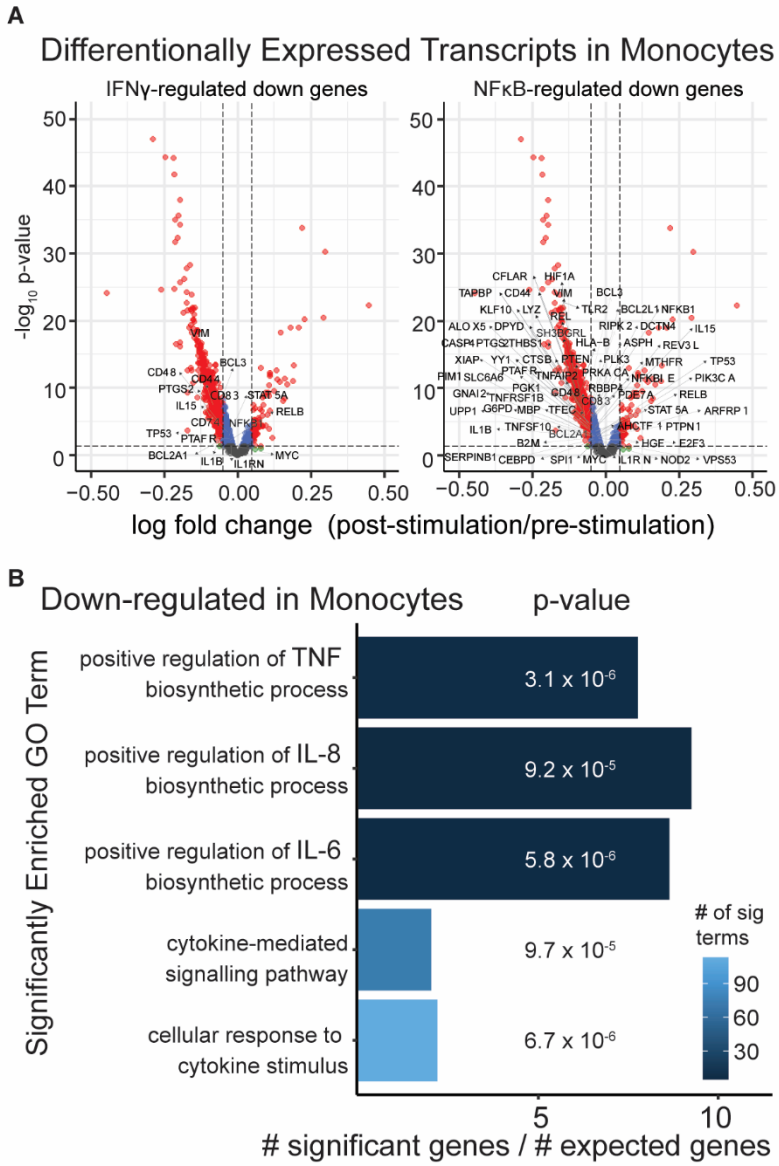


**Figure 3.** *Reduction of pro-inflammatory pathway components in monocytes with ultrasound treatment.* A) Volcano plot showing all detected genes in monocytes, highlighting differentially expressed genes (p-value <0.05) and labeled IFNγ-regulated genes that are down regulated, as well as NFκB-regulated genes that are down regulated as characterized by KEGG pathway gene lists. B) Gene ontology (GO) analysis using Bioconductor package 'topGO', determining functional GO terms significantly enriched within downregulated genes in monocytes. Enriched GO terms associated with cytokine production are shown, where bars represent number of significant genes in a list relative to number of genes that would be expected by chance, and with number of genes contributing to each GO term represented by the shade of blue. p-values for each term shown is from Fisher exact test.

with inflammation. The GO system of classification assigns genes (for differentially expressed gene list) into bins based on their functional characteristics. Gene sets can then be analyzed for GO terms that are statistically over-represented among that set, allowing for a better understanding of which biological processes (e.g., inflammation) may be changed with treatment. Out of the top statistically enriched GO terms for the down-regulated genes, we observe many that contribute to pro-inflammatory cellular processes. Genes suppressed by ultrasound show enrichment of GO terms including "inflammatory response" (p-value = 1.50 E-5, Table S3), "cytokine-mediated signaling pathway," and "cellular response to cytokine stimulus" (p-values = 9.7 E-5 and 6.7E-6, Fig. 3B). We also observe enriched GO terms associated with positive regulation of TNF, IL-6, and IL-8 among the down-regulated genes, suggesting that inducing signals for TNF or IL-6 are also suppressed, despite the absences of significant change in TNF or IL-6 transcript levels (Fig. 3B). These GO term results show that many gene transcripts encoding for cellular inflammatory functions go down after ultrasound treatment.

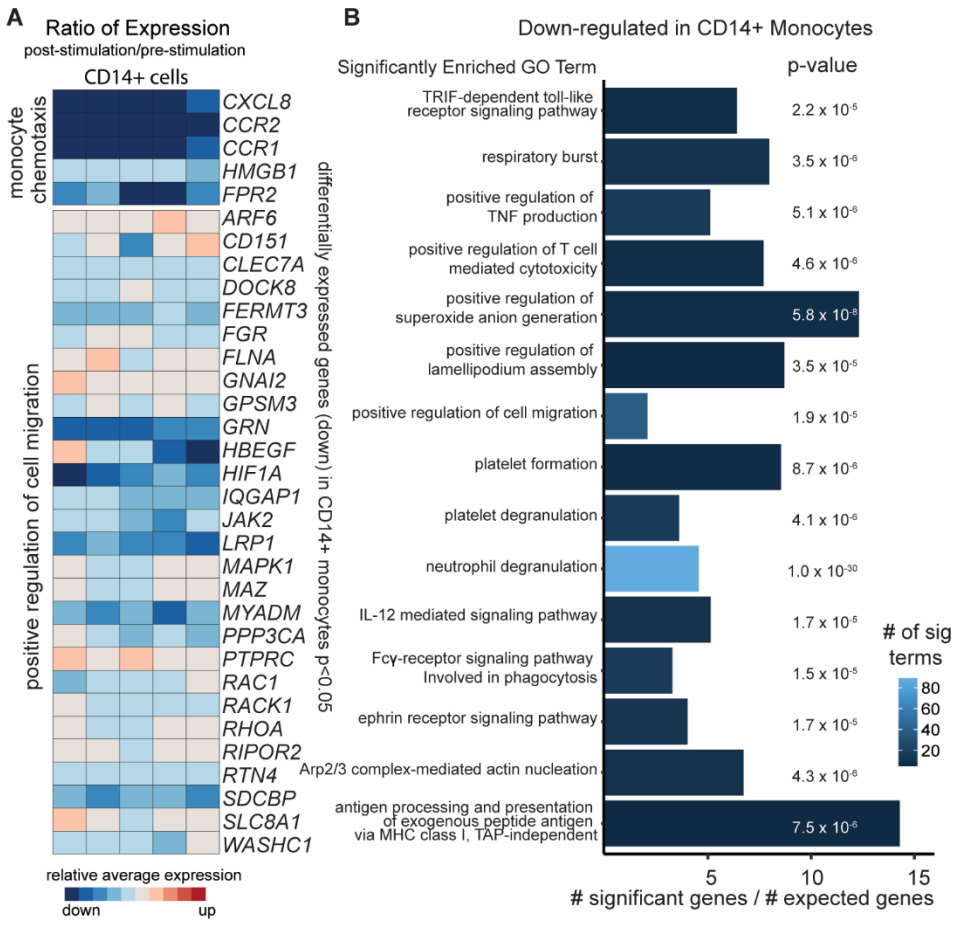


**Figure 4.** *Ultrasound results in downregulation of cellular migration components in CD14+ monocytes.* A) Heatmap displaying the average relative expression (for all cells in specified group) of significantly downregulated transcripts (genes listed on the right) for post-ultrasound compared to (divided by) pre-ultrasound levels for each subject (represented by columns, n = 5) in CD14+ cells. Genes encoding components involved in monocyte chemotaxis and cell migration are grouped and labeled to the left. B) Enriched GO terms within downregulated genes in CD14+ cells are shown, where bars represent the number of significant genes in the list relative to the number of genes that would be expected by chance, and with the number of genes contributing to each term represented by the shade of blue.. p-value for each term shown is based on Fisher exact test.

*Down-regulation of Components Involved in Monocyte Migration*

Within circulating monocytes, we observe ultrasound-treatment associated GO term enrichment of cellular components associated with IL-8 functionality (Fig. 3B), as well as a robust reduction in IL-8 across subjects (Fig. 4A, columns represent subject cell type averages). IL-8 is a chemokine (chemotactic factor), which stimulates neutrophil movement towards inflammatory sites. Therefore, we further assessed if ultrasound influences other signaling molecules involved with cellular migration (e.g., to sites of inflammation). GO term analysis of down-regulated genes in

CD14+ monocytes show enrichment of "positive regulation of cell migration" among the top 15 significantly enriched GO terms. Other GO terms, such as "lamellipodium assembly" (facilitates cell mobility), "ephrin receptor signaling" (promotes cell adhesion), and "actin nucleation" (involved with cell locomotion), all suggest that ultrasound treatment induces down regulation of genes involved with cell migration (Fig. 4B). Furthermore, genes that more specifically contribute to "monocyte chemotaxis" are down-regulated post-ultrasound stimulation in CD14+ monocytes and many of these genes are consistently reduced across all five subjects (Fig. 4A), even with quite variable or inhomogeneous patient characteristics (Table S2).

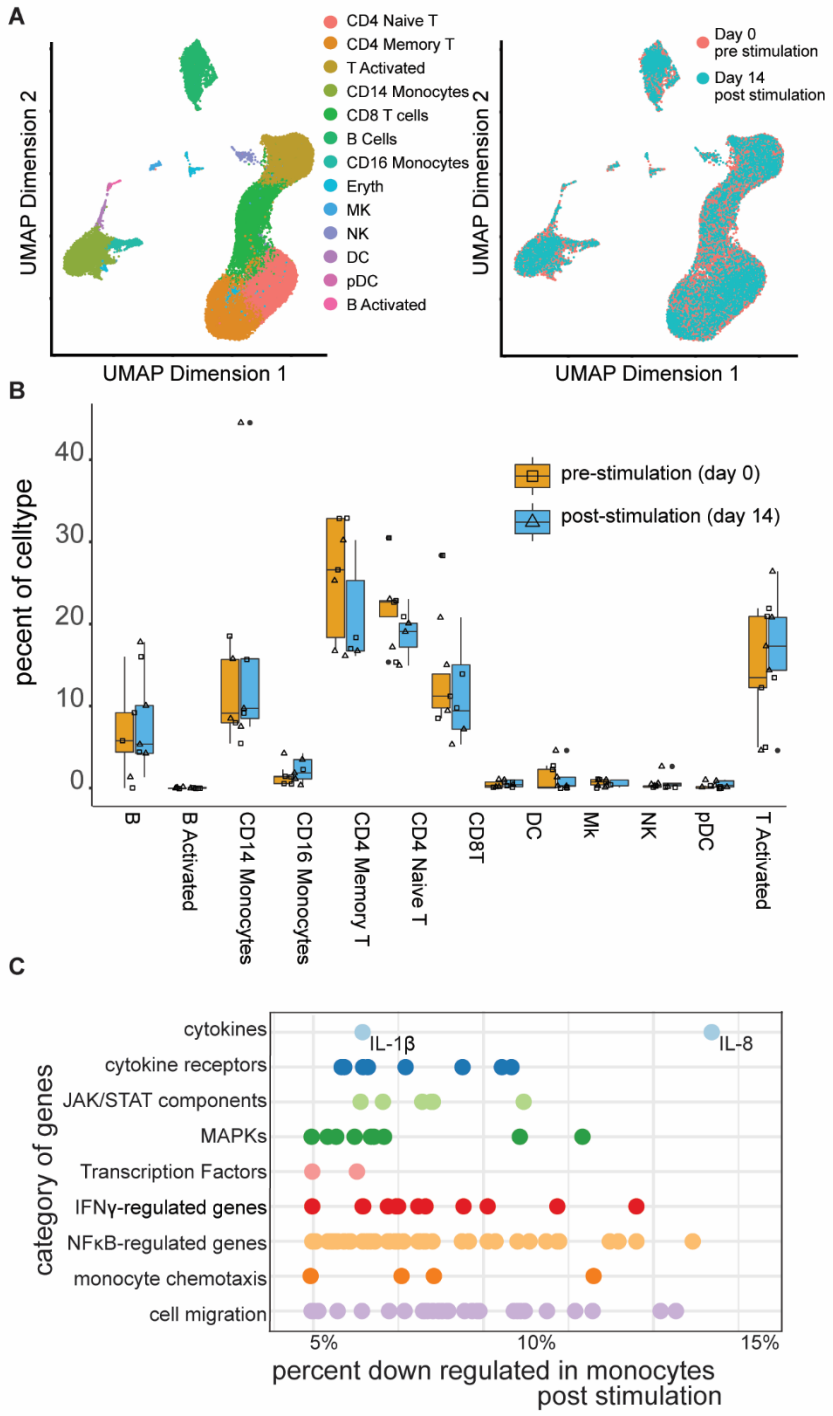


### *Immune Cell Repertoire Unchanged with Moderate Degree of Suppression*

We sought to determine how ultrasound affects the circulating immune cell repertoire. In comparing the transcriptional profiles (based on principal component analysis and UMAP dimensional reduction) of all circulating peripheral blood mononuclear cells pre- and post-ultrasound stimulation,

**Figure 5.** *Ultrasound provides a moderate effect on the immune system.* A) UMAP showing top two dimensions (principal components) contributing to variability within the dataset. All cells are shown, consisting of 53,343 cells from 10 samples (subjects = 5, timepoints = 2) with cell type and timepoint represented by color showing transcriptional signatures and relative number of cells is consistent between timepoints. B) Box plot showing median percent of each cell type (subjects, n =5) captured before ultrasound stimulation (day 0, orange, open squares) and after ultrasound stimulation (day 14, blue, open triangles) with filled in circles representing outliers. No statistical difference was detected using a paired Wilcoxon ranked-sum test (Table S4). C) Percent down regulation range is shown after 14 days of ultrasound stimulation for each gene (represented by dots) in each functional category described previously.

we observe remarkable consistency (Fig. 5A). Also, the calculated relative percent of each cell-type for each subject is displayed, and based on a paired Wilcoxon rank sum test for pre- and post-stimulation for each cell type, we observe no significant difference in the relative proportions of percent contribution of any of the 13 cell types (Fig. 5B, statistics shown in Table S4). Additionally, when comparing the number of cells sequenced for each cell type per participant there is no significant difference between timepoints (i.e. no technical bias, Table S4).

We also determined what degree of suppression occurred after ultrasound stimulation for genes involved in inflammation (genes shown in Fig. 2C, 3A and 4A). Most genes show a ~5-15% reduction in transcript levels, suggesting a moderate degree of suppression, with IL-8 and genes involved in cell migration showing the highest degree of suppression (>15%, Fig. 5C). These findings suggest that spleen-targeted ultrasound can potentially provide a way to blunt the elevated release of circulating cytokines and chemokines in inflammatory disorders or viral infections, without disrupting the overall immune cell repertoire.

*B Cells Retain Antibody Production Abilities*

One concern in treating acute hyperinflammation is that the therapy may suppress the adaptive immune response, and the ability of the immune system to provide pathogen clearance and/or protection from co-infection with a second pathogen. Therefore, we assessed whether non-invasive splenic ultrasound treatment suppresses the adaptive immune response or more specifically antibody production. Our transcriptomic data do not suggest a suppression of the adaptive immune response. In fact, we observe that among genes upregulated in B cells, there is an enrichment for GO terms associated with "B cell activation" (Fig. 6A). Genes associated with this GO term include transcripts that encode for IgA, IgG, and IgM antibodies. Interestingly, these gene transcripts are upregulated in some of the ultrasound-treated subjects (Fig. 6B), though with greater variability in results across subjects than was observed for suppression of cytokines and chemokines in monocytes. For example, we observe that for average transcript levels across B cells, transcripts encoding IgG are only upregulated in 2 or 3 subjects (*IGHG2* and *IGHG4*, respectively) out of the 5 subjects. Regardless of the variability across subjects, these data support that ultrasound treatment does not generally inhibit B cell activation and antibody production across patients, and can even potentially enhance antibody production; thus, ultrasound is not expected to compromise the adaptive immune response.

To further investigate the effects of splenic ultrasound stimulation on adaptive immune response and antibody production, as well as the variability we observed across human subjects for transcript levels that encode for IgA, IgG, and IgM antibodies, we performed additional experiments using prophylactic ultrasound stimulation (i.e., ultrasound stimulation prior to antigen exposure) in a rodent model of endotoxemia (*31*). We observe that splenic ultrasound stimulation prior to endotoxin exposure (three minutes daily, once a day for 3 days followed by LPS injection on the fourth day) results in a significant increase in IgM and IgG antibody production 24 hours after LPS exposure compared to sham and/or non-LPS controls (p-values listed in Fig. 6C description). Furthermore, this enhanced antibody output is dependent on the presence of the toxin/antigen, as there is no observed ultrasound effect on antibody production in the absence of LPS exposure. The increase in antibody transcript levels we observed in some of the human subjects, and not in the others, may be attributed to those participants also having encountered an antigen, such as a cold or other infection that was not identified during the study. This explanation is further supported by a recent report demonstrating that brain-spleen neural pathways are capable

of modulating splenic plasma cells differentiation upon presentation of novel T Cell dependent antigens (*45*).

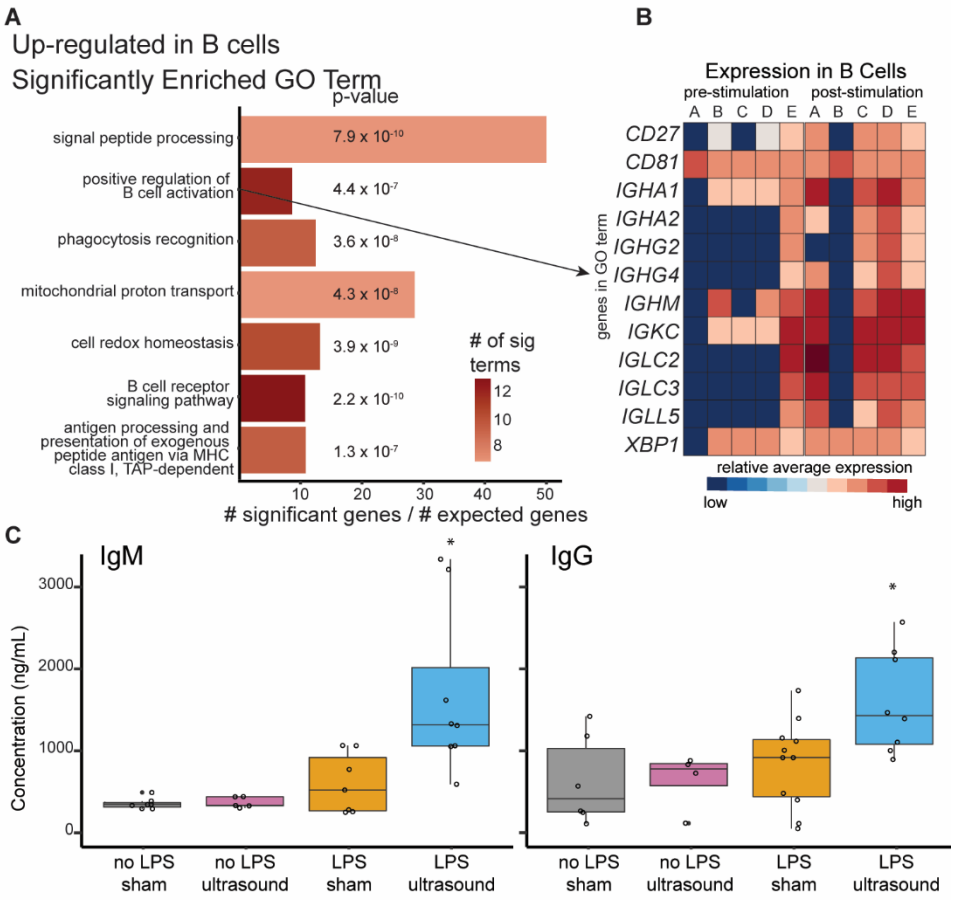


**Figure 6.** *Ultrasound treatment does not reduce adaptive immune response.* A) Enriched GO terms within upregulated genes in all B cells are shown, where bars represent number of significant genes in list relative to number of genes that would be expected by chance, and with number of genes contributing to each term represented by red hue. p-value for each term shown is based on Fisher exact test. B) Heatmap displaying genes that contribute to the GO term "positive regulation of B cell activation" within B cells. Each column represents relative average expression per subject for pre-stimulation (left 5 columns) and post-stimulation (right 5 columns) for each gene (labeled to the right). C) A rodent model of endotoxemia was used to further characterize the effects of splenic ultrasound stimulation on antibody production (further details of experiments are provided in Materials and Methods section). Box plot showing median levels of IgM (left) or IgG (right) concentrations in serum (open circles represent individual animals) for naïve animals (no LPS + sham), animals exposed to splenic ultrasound stimulation with no endotoxin (no LPS + ultrasound), animals exposed to the endotoxin but receiving sham stimulation (LPS + sham), and animals receiving both LPS exposure and splenic ultrasound stimulation (LPS + ultrasound). Animals receiving LPS + ultrasound showed significant increases in antibody production when compared to each of the other groups using an unpaired Wilcoxon ranked-sum test for IgM (no LPS + sham, $p = 0.00145$; no LPS + ultrasound, $p = 0.00155$; LPS + sham, $p = 0.01757$) and for IgG (no LPS + sham, $p = 0.02930$; no LPS + ultrasound, $p = 0.00404$; LPS + sham, $p = 0.04298$). No other comparisons using this test showed significance, $p < 0.05$.

## Discussion

By presenting the first in-human data from two independent studies using different devices and protocols, we have consistently demonstrated that non-invasive ultrasound stimulation of the spleen drives anti-inflammatory effects in the context of both an acute response in healthy subjects and a chronic inflammatory condition. In RA patients after two weeks of daily 30-minute ultrasound treatment to the spleen, there was a reduction in cytokine IL-1β and chemokine IL-8 in

circulating monocytes (Fig. 2). In healthy subjects, we also observed a significant reduction in TNF levels produced by *ex vivo* LPS-stimulated whole blood, in individuals stimulated with 3 minutes of pulsed ultrasound (Fig. 1B).

In addition to the reduction of cytokines, we observed a reduction in activation of multiple signaling pathways in circulating monocytes with ultrasound treatment. Cytokines signal by binding to cell surface receptors to set off a cascade of intracellular events. Important cytokines in the context of RA include TNF, IL-6, and IL-1β; their downstream intracellular pathways and necessary signaling molecules include cytokine receptors, components of the JAK/STAT pathway, MAP kinases and NFκB (*46*, *47*). Many of the transcripts that encode for these critical components are downregulated with ultrasound treatment in RA patients (Fig. 2B). This finding suggests that in addition to cytokines and their immediate receptors, there is broad suppression of cellular pro-inflammatory pathways.

Down regulation of these various pro-inflammatory transcripts in RA patients occurs in the context of chronic inflammation. However, these same pathways are also involved in acute inflammatory responses (*47*). Genes induced by LPS-stimulated human monocytes include TNF, IL-1, IL-6, and IL-8 (*48*). NFκB and associated pathways are also upregulated, and NFκB is activated via phosphorylation during LPS exposure, allowing for a rapid induction of genes so the system can respond in an acute inflammatory setting. These same cellular components are downregulated with ultrasound treatment in our RA patients, suggesting that non-invasive splenic ultrasound could be used clinically to suppress acute inflammation as well.

The discovery that splenic ultrasound can reduce or calm an overactive innate immune response in humans is quite timely. Many of the same key inflammatory cytokines that are reduced with ultrasound stimulation are elevated in COVID-19 patients. Recent studies have revealed that COVID-19 patients consistently produce high levels of IL-1β, IL-8, IL-6, and TNF, which strongly suggests dysregulation in the innate immune response (*34-37*). More specifically, SARS-CoV-2 infected individuals exhibit significantly higher expression levels of IL-1β and IL-6 transcripts in circulating monocytes, as well as IFNγ in CD8+ T cells, shown through PBMC single-cell RNA sequencing of COVID-19 patients (*38*). Single cell RNA sequencing has further shown that bronchoalveolar lavage fluid from patients with severe COVID-19 disease have higher levels of IL-8, IL-6 and IL-1β compared to patients with only moderate disease (*49*). These molecules are key components of the COVID-19 cytokine storm that function in acute lung injury to recruit neutrophils to alveoli, inducing lung tissue damage (*39*). Recently, SARS-CoV-2 infection in children has been associated with a novel multisystem inflammatory disease (MIS-C) resembling toxic shock syndrome or atypical Kawasaki disease (*50*). Kawasaki disease also presents with elevated transcripts levels of genes encoding for IL-1, IL-6, IL-8, and IL-17 (*51*); and along with ARDS, is likely to be a condition caused by the COVID-19-induced cytokine storm (*52*). Clinical therapies that can suppress these pro-inflammatory cytokines and reduce migration of circulating immune cells to the lungs may be capable of treating patients with moderate to severe cases of COVID-19 to calm the cytokine storm and prevent morbidity and mortality (Fig. 7A).

Ultrasound has the potential to prevent or improve severe symptoms associated with the cytokine storm in COVID-19 patients. In addition to demonstrating the ability to reduce key pro-inflammatory cytokines and signaling pathways involved with a hyperactive innate immune response, splenic ultrasound also reduces IL-8 and many components associated with cell migration, specifically monocyte migration (Fig. 4). These findings are consistent with previous animal studies showing that activation of the cholinergic anti-inflammatory pathway suppresses

monocyte migration in mice (*46*). Taken together, one proposed mechanism of action for ultrasound treatment is that ultrasound modulates circulating immune cells initially within the spleen via activation of the cholinergic anti-inflammatory pathway, which suppresses pro-inflammatory cytokines and signaling pathways, as well as inhibiting cellular migration, such that there is reduced inflammation at the target site (e.g., at joints in RA or alveoli for COVID-19; Fig. 7A). Furthermore, data in humans and pre-clinical animal data show an increase in antibody production with splenic ultrasound. These results demonstrate an advantageous feature of splenic ultrasound compared to pharmaceutical options for immunosuppression, such as TNF, IL-6, or IL-1 blocking biologics (*39, 40*), in that cytokine suppression does not inhibit other functions of the adaptive immune system, such as B cell activity or antibody production. Indeed, splenic ultrasound may enhance the adaptive immune system through the recently discovered brain-spleen neuroimmune pathway that enhances differentiation of antibody-producing splenic plasma cells (SPPCs) upon antigen activation (*45*).

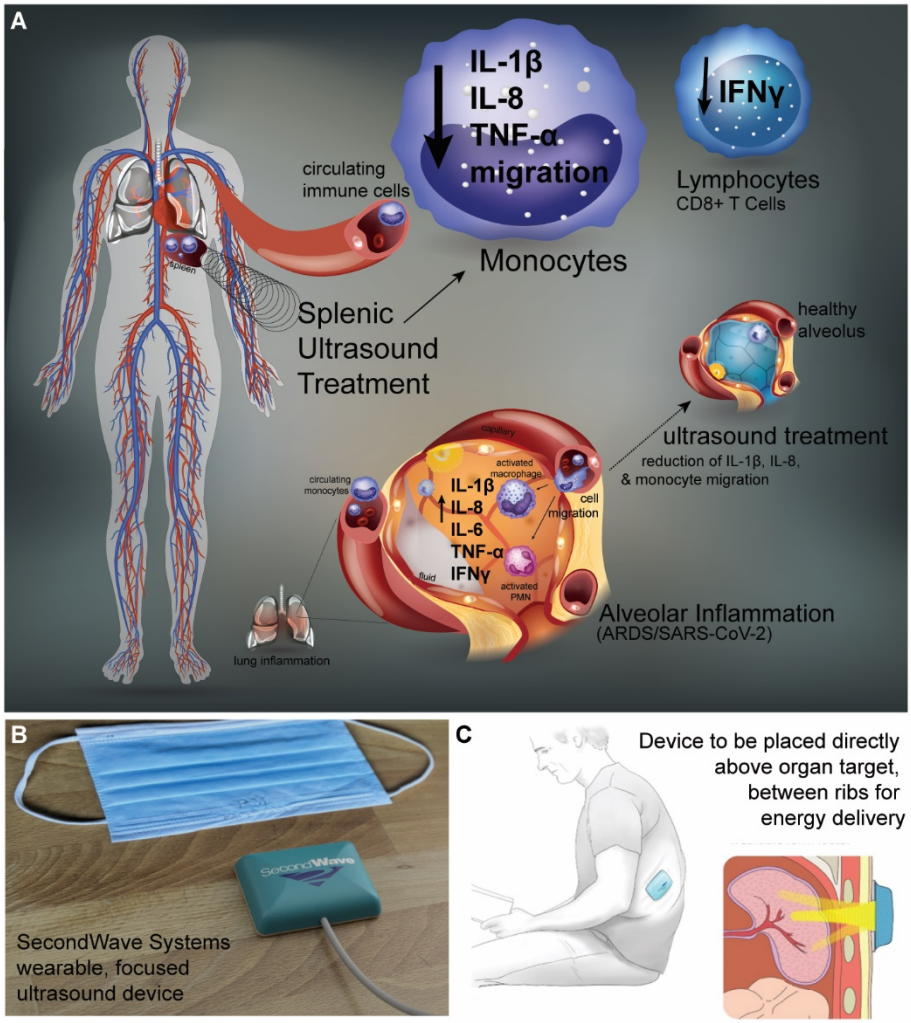


**Figure 7.** *Non-invasive splenic ultrasound treatment for ameliorating immune hyperactivity for COVID-19*. A) Schematic of the proposed mechanism of splenic ultrasound treatment's effect on circulating immune cells. Splenic ultrasound reduces IL-1β, IL-8, TNF and likely monocyte migration to areas of inflammation (data supporting this model shown here, solid arrow). This treatment approach could help combat key elevated cytokines in alveoli and/or cellular migration to lungs in the context of COVID-19 (dashed arrow). B) A new wearable phased-array ultrasound device developed by SecondWave Systems (Minneapolis, Minnesota) designed specifically for splenic stimulation to treat COVID-19 patients. C) The SecondWave device is positioned over the ribs area and ultrasound energy is steered and focused to target the spleen for daily treatment (e.g., 10 minutes of stimulation per session).

One limitation of the presented results in the context of COVID-19 or a cytokine storm is that ultrasound stimulation of the spleen may not generate anti-inflammatory effects sufficient to suppress a severe infectious inflammatory response. The anti-inflammatory effects in this paper in response to splenic ultrasound were demonstrated acutely (single 3-minute stimulation) in healthy human subjects or to a moderate extent in RA patients. The question remains whether the anti-inflammatory effects observed in healthy subjects or in patients with a chronic inflammation disorder, such as RA, will translate to patients harboring a systemic viral infection, as observed for COVID-19. This question will be answered through a clinical trial that is currently being set up at the University of Minnesota together with GE Research to test this ultrasound approach in COVID-19 patients funded by the Defense Advanced Research Projects Agency (DARPA; Department of Defense).

One key asset of the upcoming COVID-19 study is that GE's cart-based ultrasound system (GE LOGIQ E10) with enhanced targeting capabilities will be used on patients. In the ongoing RA study at the University of Minnesota, a commercially available ultrasound device (SoundCare Plus) was used on patients that did not have targeting capabilities tailored for the spleen. At the onset of that RA study, SoundCare Plus was one of few devices that was already FDA regulated for various stimulation applications; thus, this unit was selected for the RA study. The GE LOGIQ E10 device can be used to better target and stimulate specific locations of the spleen, which the GE team has already demonstrated with strong anti-inflammatory effects in healthy human subjects (Fig. 1B). Previous animal studies have also demonstrated that stronger anti-inflammatory effects are possible with better focusing of stimulation within the spleen or longer periods on a given target (*31, 32*). Furthermore, sufficient activation of the cholinergic anti-inflammatory pathway has been shown to combat acute and deadly cytokine storm conditions in sepsis animal models, and the magnitude of cytokine suppression provided by ultrasound is consistent with the protection provided by implant-based or pharmaceutical methods in these studies (*31, 53, 54*).

In parallel with the DARPA-funded study, both GE and a start-up company, SecondWave Systems, are developing wearable or portable ultrasound systems for neuromodulation (Fig. 7B) that can be positioned over the rib to steer and focus ultrasound energy to different locations of the spleen or other organ targets (Fig. 7C). Both GE and SecondWave are currently organizing clinical studies at multiples sites worldwide to assess the safety and feasibility of their therapeutic ultrasound devices. Success with these initial clinical studies will propel further development and scale-up efforts for splenic ultrasound technologies to meet the large-scale demand for COVID-19, as well as open up opportunities to treat future viral infections and other inflammatory disorders in combination with or in lieu of biologics.

## Materials and Methods

### *Splenic ultrasound in healthy subjects: Design of clinical study*

For the splenic ultrasound study involving healthy human subjects (clinicaltrials.gov: NCT03548116), we provide the data from the two cohorts most relevant to the planned DARPA sponsored COVID study: the sham control cohort (i.e., no ultrasound, with only mechanical pressure over the spleen) and a splenic ultrasound stimulation cohort (i.e., 290.4 mW/cm$^2$ $I_{SPTA}$ or 1.4 mechanical index (MI) using the shear wave elastography setting on GE LOGIQ E9) that insonified a single site (i.e., the splenic hilum; as identified by a trained ultrasonographer performing the stimulation). The trial was carried out in accordance with International Conference

on Harmonisation Good Clinical Practice (ICH GCP) and the United States Code of Federal Regulations (CFR) applicable to clinical studies (45 CFR Part 46, 21 CFR Part 50, 21 CFR Part 56, and 21 CFR Part 812). The protocol, informed consent form, recruitment materials, and all participant materials were submitted and approved by the Institutional Review Board (IRB) at Northwell Health.

*Inclusion and exclusion criteria.* To be eligible to participate in the study, an individual must have met the following criteria: aged between 18 and 45 years, be without physical disability or conditions that may make them incapable of undergoing the study procedures or otherwise place them at greater harm, be without significant past medical or surgical histories that would render them at a greater risk of harm, be considered English proficient due to the study requirement to follow verbal commands during the ultrasound session, be considered active as assessed by type of activity (e.g., walking or running) and number of hours a week performing the various activities, be able to attend all study visits at approximately the same time of day, be able to comprehend the study goals and procedures, and able to provide informed consent for participation. See Table S5 for subject characteristics used in the cytokine analysis shown in Fig. 1.

*Study timeline.* Subjects underwent a screening visit 1 to 11 days prior to baseline visit to assess eligibility to participate in the study. Eligible individuals that agreed to participate and provided written informed consent then underwent a physical and neurological examination. Women of childbearing potential were asked to provide a urine sample for pregnancy testing, and approximately 21 mL of blood was drawn. On the first protocol visit (day 0), participants again underwent a physical and neurological examination, and medical history review. A baseline blood draw was then collected for cytokine and blood chemistry analysis (~35 mL). The blood draw was performed under sterile conditions using standard venipuncture techniques. Individuals then underwent the ultrasound procedure based on random assignment to one of 7 groups, including the two groups reported herein (i.e., the sham control group, and a stimulated group that received 100% power stimulus applied at a single splenic target location). For ultrasound stimulus delivery, individuals were asked to lie in the right lateral recumbent position with their arms above their heads to expose the splenic region of the abdomen. After ultrasound gel was applied to the region, the ultrasound probe was placed on the participant's abdomen. This procedure was performed for both the sham control group (n=9) and ultrasound stimulated group (n=9). Note that one subject from each group was excluded, in which 10 subjects were initially recruited to the study for each group (see Table S5).

*Stimulation paradigm.* In the ultrasound stimulated cohort, the subject had the dimensions of their spleen assessed (using the B mode imaging setting on the GE LOGIQ E9), and the probe (C1-6) was positioned over the splenic hilum. Stimulation was performed using a modified elastography setting on the LOGIQ E9 operated in two modes: an imaging/targeting mode with short ultrasound pulses (on the order of 1 microsecond) and relatively low acoustic power levels (on the order of 10 mW/cm$^2$), and a stimulation mode (from the clinical shear wave elastography setting) using longer ultrasound pulses (on the order of 1 ms) and higher acoustic power levels (290.4 mW/cm$^2$). Stimulation was performed in twelve 15-second long epochs separated by 15 seconds each, and a total stimulation duration of 3 minutes. The 15 second epochs were performed during breath holds, during which an ultrasonographer was holding the probe in position above the spleen. Before each stimulation period, the ultrasonographer checked the location of the probe using the imaging mode to ensure that all stimulation pulses were on target. The focal landmark used for targeting and stimulation was the hilum of the spleen in the group included in the presented analysis. For the

sham control group, the movements and probe contact for the ultrasound procedure were performed by the ultrasonographer, and the total duration of the procedure remained the same as the stimulated group, except that no ultrasound power was applied (i.e., ultrasound output via the probe was turned off). A post-ultrasound blood draw was again performed, and the 2-hour blood draw time-point data is reported herein.

*Blood analysis procedures.* Prior to the *ex vivo* cytokine test, the LPS was sonicated for 30 minutes. A 10 mL blood tube (heparin; green cap) was brought into a tissue culture/sterile room and blood was transferred to a 50 mL conical tube. A blinded researcher then diluted the LPS to the test concentrations in 15 pre-labeled tubes containing replicates of the different concentrations of LPS used for blood exposure (dilutions were made to achieve 0, 0.1, 1, and 10 ng/mL of LPS when mixed with blood). Upon mixing the LPS with blood, the final tubes were capped and placed on a rocker within an incubator and the samples were kept at 37 degrees Celsius for 4 hours during incubation. After the incubation, the samples were removed from the incubator, centrifuged at 6000 RPM for 5 minutes, and the plasma supernatant was transferred (via pipette) for storage (frozen prior to analysis). TNF analysis was performed in triplicate from each sample using DuoSet ELISA kit (R&D Systems), as per manufacturer's instructions.

***Splenic ultrasound in RA patients: Design of clinical study***

This clinical study is a controlled, randomized, double-blinded trial of short-term (14 days) treatment and is listed at clinicaltrials.gov (NCT03690466) for which a portion of the results are presented in this paper. The study is still ongoing, but the RNAseq data obtained thus far in five ultrasound stimulated patients is presented in this paper for its relevance in revealing the use of splenic ultrasound for potentially treating COVID-19 patients. The protocol, informed consent form, recruitment materials, and all participant materials were submitted and approved by the University of Minnesota's Institutional Review Board (IRB) and monitored by CTSI in accordance with its institutionally approved monitoring plan. The overall objective of the clinical trial is to demonstrate safety and efficacy of spleen ultrasound stimulation in the treatment of RA in 20 participants. For this ongoing study, 17 participants have been recruited, consented, and enrolled with all 17 patients completing the full study. The 17th participant completed the study, however the last 'in-clinic' visit was performed using clinician video conferencing due to the COVID-19 pandemic, while in-person blood sample collection was still able to be performed. Further details for this study can be found on clincialtrials.gov and will be presented in a future publication with complete outcome analyses. The description below only includes relevant methods and RNAseq analyses presented specifically in this paper.

*Inclusion and exclusion criteria.* To be eligible to participate in the study, an individual must have met the following criteria: 18 years of age or older, carried a diagnosis of seropositive (rheumatoid factor- or cyclic citrullinated peptide antibody-positive) rheumatoid arthritis (RA), and exhibited symptoms or signs of inadequate disease control (either modified HAQ score >0.3 or DAS-28-CRP >3.2). Exclusion criteria included active bacterial or viral infection, pregnancy, malignancy, or inability to provide daily self-care. The patient medical history and characteristics for each of the five subjects presented in this paper is provided in Table S2.

*Study timeline.* Participants were assessed during in-clinic visits on days 0 (before treatment began), 3, 7, 10, 14, and 21. Minor flexibility was allowed for scheduling clinic visits outside of holidays for special circumstances. On the first visit, the spleen was imaged by an ultrasonographer and the center of the spleen trajectory was marked on the participant's skin. Participants were

instructed on how to self-administer ultrasound treatment to the spleen. The procedure involved sweeping the ultrasound wand continuously across a 5-inch by 5-inch square centered on the spleen mark placed by the ultrasonographer and ensuring full contact was made with the skin during the daily 30 minute stimulation period. Researchers were able to visually confirm that daily treatments were administered through daily online video sessions with the patients. These video sessions took place at about the same time each day for the 14-day treatment period. With each in-clinic visit, participants received a joint examination, peripheral joint ultrasound, and blood draw, as well as completing several physical evaluations and questionnaires. Full study details including analysis of all patients and assessments will be presented in a future publication.

*Treatment.* After an in-clinic training session on Day 0, transcutaneous ultrasound was administered to the spleen for 30 minutes daily for 2 weeks (14 days total) via a portable device (1.2 W/cm$^2$; SoundCare Plus, Roscoe Medical) in the patient's home. The patients were randomized (1:1) to a treatment group or a control (sham) group, in which the latter received the exact same evaluations and stimulation paradigm as the treatment group, except that the device did not deliver any energy from the ultrasound transducer. RA patients and clinical assessors were blinded as to which patients received ultrasound or sham treatment.

*RNA-sequencing and statistical analyses.* 4mL of blood was collected in a green top LiHep tube from each ultrasound stimulated participant (n=5) on day 0 (before the first splenic ultrasound stimulation was administered) and on day 14 (after the final treatment session). The samples were processed the same day as collection. Peripheral blood mononuclear cells were isolated from whole blood using density gradient centrifugation via SepMate tubes (Stemcell Technologies) and following manufacturer's instructions. PBMCs were then gently frozen and stored at -80 ºC as per 10X Genomics demonstrated protocols GC000039. Following this protocol, once all samples had been collected and frozen, samples were thawed quickly in 20% FBS in PBS, resuspended in 10% FBS, and strained before proceeding to 10X genomics single cell protocol. Samples were sequenced using UMI-based approach from10X Genomics, as previously described (*32*) and mapped to the human genome.

Transcriptomic analysis was performed using R statistical software, and primary filtering and normalization of each sample was done using Seurat package as previously described (*32, 55, 56*). Samples included two timepoints from five subjects and these individual samples were merged for cell type assignment and differential expression analysis. Cell types were assigned using standard marker genes (see Fig. S2) as previously described (*57*). Differential expression was determined between timepoints for all cells in each cell type using a negative binomial generalized linear model. GO term analysis was performed using the org.Hs.eg.db and topGO packages. GO term enrichment was assessed using the 'elim' algorithm with a Fisher exact test cutoff of 0.01, in which the top 40 significant GO terms in monocytes are shown in Table S3 (*58*).

***Pre-clinical tests in LPS/endotoxin rodent model***

Pre-clinical tests in rodents were performed as previously described (*31*). Experiments were performed under protocols approved by the Institutional Animal Care and Use Committee of GE Research. Briefly, a VIVID E9 (GE) ultrasound system was used to perform an ultrasound scan and locate the spleen. A HIFU transducer and system was then positioned on the target area, and a separate ultrasound scan performed using a smaller probe (3S, GE) that was placed within the opening of the HIFU transducer was used to verify alignment of the ultrasound beam with the spleen. Adult Sprague-Dawley rats that were 8-12 weeks old (250-300 g; Charles River Labs) were

housed at 25 degrees Celsius on a 12-h light/dark cycle and acclimatized for 1 week, with handling before experiments to minimize the potential confounding measures due to stress response. Water and regular rodent chow were available ad libitum. LPS (0111:B4, Sigma Aldrich) was used to produce a significant state of inflammation in the naïve adult rodents. LPS was administered to animals in the amount of 10 mg/kg, which corresponds to a LD75 dose via intraperitoneal injection.

*Treatment.* For ultrasound stimulation, animals were anesthetized with 2-4% isoflurane, and the animals were laid on a water circulating warming pad to prevent hyperthermia during the procedures. The region designated for ultrasound stimulation was shaved with a disposable razor and animal clippers prior to stimulation. Ultrasound was applied to the designated area above the spleen using the probe and system described and calibrated from a previous study (*31*). An ultrasound stimulus using the previously found optimal stimulation parameters (1.1 MHz, 0.5 ms pulse repetition frequency, 136.36 microsecond pulse length, 568 mW/cm$^2$ $I_{SPTA}$) was then applied for 2 minutes, and LPS was immediately injected post-stimulation. Animals were allowed to incubate under anesthesia for one hour, and after incubation the animal was euthanized, and tissue and blood samples were collected. For experiments testing antibody production, an ultrasound stimulus was applied daily (in the morning) for three days prior to LPS injection. On the fourth day, following the three consecutive treatment days, LPS (10mg/kg) was injected intraperitoneally. The animals were then incubated for 60 minutes in accordance with previous studies, and tissue and blood were harvested for analysis of cytokines and antibody production.

*Tissue collection.* An incision was made starting at the base of the peritoneal cavity extending up and through to the pleural cavity. The spleen was rapidly removed and homogenized in a solution of phosphate-buffered saline, containing phosphatase (0.2-mM phenylmethylsulfonyl fluoride, 5-µg/mL aprotinin, 1-mM benzamidine, 1-mM sodium orthovanadate, and 2-µM cantharidin) and protease (1-µL to 20 mg of tissue as per Roche Diagnostics) inhibitors. A targeted final concentration of 0.2-g tissue per mL PBS solution was applied in all samples. After collection of the whole blood, we allowed the blood to clot undisturbed at room temperature for 15–30 minutes. Samples were centrifuged at 1,000–2,000x g for 10 minutes in a refrigerated centrifuge with the resulting supernatant being collected for antibody testing. Samples were then stored at −80 °C until analysis. Splenic tissue lysate was analyzed for cytokine concentrations using ELISA kits for quantifying TNF alpha (Abcam, Ab100785), IFN gamma (Abcam, Ab239425), IL-13 (Abcam, Ab100766), IL-12 (LSBio, LS-F34357), IL-10 (Abcam, Ab100765), IL-2 (Abcam, Ab221834), IL-1 beta (Abcam, Ab100768), IL-1 alpha (Abcam, Ab113350), IL-6 (Abcam, Ab234570) and IL-4 (Abcam, Ab100771) as per manufacturer's instructions for tissue samples. Serum was tested using ELISA kits for quantifying antibody production including IgG (Abcam, Ab189578), and IgM (Abcam, Ab215085) as per manufacturer's instructions.

## References:


1. T. S. Xiao, Innate immunity and inflammation. *Cell Mol Immunol* **14**, 1-3 (2017).
2. K. Newton, V. M. Dixit, Signaling in innate immunity and inflammation. *Cold Spring Harb Perspect Biol* **4**, (2012).
3. S. Koyama, K. J. Ishii, C. Coban, S. Akira, Innate immune response to viral infection. *Cytokine* **43**, 336-341 (2008).
4. S. S. Chavan, V. A. Pavlov, K. J. Tracey, Mechanisms and Therapeutic Relevance of Neuro-immune Communication. *Immunity* **46**, 927-942 (2017).
5. X. Li, X. Ma, Acute respiratory failure in COVID-19: is it "typical" ARDS? *Crit Care* **24**, 198 (2020).
6. N. Chen *et al.*, Epidemiological and clinical characteristics of 99 cases of 2019 novel coronavirus pneumonia in Wuhan, China: a descriptive study. *Lancet* **395**, 507-513 (2020).
7. M. Bosmann, P. A. Ward, The inflammatory response in sepsis. *Trends Immunol* **34**, 129-136 (2013).
8. G. R. Kinsey, L. Li, M. D. Okusa, Inflammation in acute kidney injury. *Nephron Exp Nephrol* **109**, e102-107 (2008).
9. D. Aletaha *et al.*, 2010 Rheumatoid arthritis classification criteria: an American College of Rheumatology/European League Against Rheumatism collaborative initiative. *Arthritis Rheum* **62**, 2569-2581 (2010).
10. P. Enck *et al.*, Irritable bowel syndrome. *Nat Rev Dis Primers* **2**, 16014 (2016).
11. P. S. Olofsson, K. J. Tracey, Bioelectronic medicine: technology targeting molecular mechanisms for therapy. *J Intern Med* **282**, 3-4 (2017).
12. K. Birmingham *et al.*, Bioelectronic medicines: a research roadmap. *Nat Rev Drug Discov* **13**, 399-400 (2014).
13. K. J. Tracey, The inflammatory reflex. *Nature* **420**, 853-859 (2002).
14. U. Andersson, K. J. Tracey, Neural reflexes in inflammation and immunity. *J Exp Med* **209**, 1057-1068 (2012).
15. V. A. Pavlov, S. S. Chavan, K. J. Tracey, Molecular and Functional Neuroscience in Immunity. *Annu Rev Immunol* **36**, 783-812 (2018).
16. T. Inoue *et al.*, Vagus nerve stimulation mediates protection from kidney ischemia-reperfusion injury through alpha7nAChR+ splenocytes. *J Clin Invest* **126**, 1939-1952 (2016).
17. M. Rosas-Ballina *et al.*, Splenic nerve is required for cholinergic antiinflammatory pathway control of TNF in endotoxemia. *Proc Natl Acad Sci U S A* **105**, 11008-11013 (2008).
18. F. A. Koopman *et al.*, Vagus nerve stimulation inhibits cytokine production and attenuates disease severity in rheumatoid arthritis. *Proc Natl Acad Sci U S A* **113**, 8284-8289 (2016).
19. L. V. Borovikova *et al.*, Vagus nerve stimulation attenuates the systemic inflammatory response to endotoxin. *Nature* **405**, 458-462 (2000).
20. L. G. Reys *et al.*, Uncovering the neuroenteric-pulmonary axis: vagal nerve stimulation prevents acute lung injury following hemorrhagic shock. *Life Sci* **92**, 783-792 (2013).
21. Y. Lai *et al.*, Vagus nerve stimulation protects against acute liver injury induced by renal ischemia reperfusion via antioxidant stress and anti-inflammation. *Biomed Pharmacother* **117**, 109062 (2019).
22. N. Thompson, S. Mastitskaya, D. Holder, Avoiding off-target effects in electrical stimulation of the cervical vagus nerve: Neuroanatomical tracing techniques to study fascicular anatomy of the vagus nerve. *J Neurosci Methods* **325**, 108325 (2019).
23. D. P. Darrow, P. O'Brien, T. J. Richner, T. I. Netoff, E. S. Ebbini, Reversible neuroinhibition by focused ultrasound is mediated by a thermal mechanism. *Brain Stimul* **12**, 1439-1447 (2019).
24. N. Wattiez *et al.*, Transcranial ultrasonic stimulation modulates single-neuron discharge in macaques performing an antisaccade task. *Brain Stimul* **10**, 1024-1031 (2017).
25. J. Kubanek *et al.*, Remote, brain region–specific control of choice behavior with ultrasonic waves. *Science Advances* **6**, eaaz4193 (2020).
26. P. P. Lele, Effects of focused ultrasonic radiation on peripheral nerve, with observations on local heating. *Experimental Neurology* **8**, 47 - 83 (1963).
27. H. Guo *et al.*, Ultrasound Produces Extensive Brain Activation via a Cochlear Pathway. *Neuron* **99**, 866 (2018).
28. S. J. Ilham *et al.*, single-unit recordings reveal increased peripheral nerve conduction velocity by focused pulsed ultrasound. *Biomed Phys Eng Express* **4**, (2018).
29. J. C. Gigliotti *et al.*, Ultrasound Modulates the Splenic Neuroimmune Axis in Attenuating AKI. *J Am Soc Nephrol* **26**, 2470-2481 (2015).

30. V. Cotero *et al.*, Peripheral Focused Ultrasound Stimulation (pFUS): New Competitor in Pharmaceutical Markets? *SLAS Technol* **24**, 448-452 (2019).
31. V. Cotero *et al.*, Noninvasive sub-organ ultrasound stimulation for targeted neuromodulation. *Nat Commun* **10**, 952 (2019).
32. D. P. Zachs *et al.*, Noninvasive ultrasound stimulation of the spleen to treat inflammatory arthritis. *Nat Commun* **10**, 951 (2019).
33. N. S. Nunes *et al.*, Therapeutic ultrasound attenuates DSS-induced colitis through the cholinergic anti-inflammatory pathway. *EBioMedicine* **45**, 495-510 (2019).
34. J. C. Gigliotti *et al.*, Ultrasound prevents renal ischemia-reperfusion injury by stimulating the splenic cholinergic anti-inflammatory pathway. *J Am Soc Nephrol* **24**, 1451-1460 (2013).
35. C. Pasquinelli, L. G. Hanson, H. R. Siebner, H. J. Lee, A. Thielscher, Safety of transcranial focused ultrasound stimulation: A systematic review of the state of knowledge from both human and animal studies. *Brain Stimul* **12**, 1367-1380 (2019).
36. M. M. Doyley, K. J. Parker, Elastography: general principles and clincial applications. *Ultrasound Clin* **9**, 1-11 (2014).
37. K. Whalley, Brain-spleen link tunes immunity. *Nat Rev Immunol*, (2020).
38. J. Dalli, R. A. Colas, H. Arnardottir, C. N. Serhan, Vagal Regulation of Group 3 Innate Lymphoid Cells and the Immunoresolvent PCTR1 Controls Infection Resolution. *Immunity* **46**, 92-105 (2017).
39. M. Fernandez-Ruiz, J. M. Aguado, Risk of infection associated with anti-TNF-alpha therapy. *Expert Rev Anti Infect Ther* **16**, 939-956 (2018).
40. V. R. Lang *et al.*, Risk of infections in rheumatoid arthritis patients treated with tocilizumab. *Rheumatology (Oxford)* **51**, 852-857 (2012).
41. R. Torres-Rosas *et al.*, Dopamine mediates vagal modulation of the immune system by electroacupuncture. *Nat Med* **20**, 291-295 (2014).
42. A. Bruchfeld *et al.*, Whole blood cytokine attenuation by cholinergic agonists ex vivo and relationship to vagus nerve activity in rheumatoid arthritis. *J Intern Med* **268**, 94-101 (2010).
43. X. Wittebole *et al.*, Nicotine exposure alters in vivo human responses to endotoxin. *Clin Exp Immunol* **147**, 28-34 (2007).
44. K. J. Tracey, Physiology and immunology of the cholinergic antiinflammatory pathway. *J Clin Invest* **117**, 289-296 (2007).
45. X. Zhang *et al.*, Brain control of humoral immune responses amenable to behavioural modulation. *Nature* **581**, 204-208 (2020).
46. M. Noack, P. Miossec, Selected cytokine pathways in rheumatoid arthritis. *Semin Immunopathol* **39**, 365-383 (2017).
47. C. A. Feghali, T. M. Wright, Cytokines in acute and chronic inflammation. *Front Biosci* **2**, d12-26 (1997).
48. M. Guha, N. Mackman, LPS induction of gene expression in human monocytes. *Cell Signal* **13**, 85-94 (2001).
49. M. Liao *et al.*, Single-cell landscape of bronchoalveolar immune cells in patients with COVID-19. *Nat Med*, (2020).
50. Z. Belhadjer *et al.*, Acute heart failure in multisystem inflammatory syndrome in children (MIS-C) in the context of global SARS-CoV-2 pandemic. *Circulation*, (2020).
51. S. Menikou, P. R. Langford, M. Levin, Kawasaki Disease: The Role of Immune Complexes Revisited. *Front Immunol* **10**, 1156 (2019).
52. A. Alunno, F. Carubbi, J. Rodriguez-Carrio, Storm, typhoon, cyclone or hurricane in patients with COVID-19? Beware of the same storm that has a different origin. *RMD Open* **6**, (2020).
53. A. Kanashiro *et al.*, Therapeutic potential and limitations of cholinergic anti-inflammatory pathway in sepsis. *Pharmacol Res* **117**, 1-8 (2017).
54. H. Wang *et al.*, Cholinergic agonists inhibit HMGB1 release and improve survival in experimental sepsis. *Nat Med* **10**, 1216-1221 (2004).
55. A. Butler, P. Hoffman, P. Smibert, E. Papalexi, R. Satija, Integrating single-cell transcriptomic data across different conditions, technologies, and species. *Nat Biotechnol* **36**, 411-420 (2018).
56. T. Stuart *et al.*, Comprehensive Integration of Single-Cell Data. *Cell* **177**, 1888-1902 e1821 (2019).
57. H. M. Kang *et al.*, Multiplexed droplet single-cell RNA-sequencing using natural genetic variation. *Nat Biotechnol* **36**, 89-94 (2018).
58. A. Alexa, J. Rahnenfuhrer, T. Lengauer, Improved scoring of functional groups from gene expression data by decorrelating GO graph structure. *Bioinformatics* **22**, 1600-1607 (2006).

**Acknowledgments:** We thank all study participants. We are grateful for the assistance of individuals at the University of Minnesota Genomics Center, especially Jerry Daniel and Emma Stanley. Additionally, we would like to thank Stuart Sealfon and Frederique Ruf-zamojski for their assistance and advice processing PBMC samples for single cell sequencing. This work was supported by the United States Defense Advanced Research Projects Agency (DARPA) Electrical Prescriptions (ElectRx) Program under the guidance of Eric Van Gieson and Gretchen Knaack at DARPA. The views, opinions and/or findings expressed are those of the authors and should not be interpreted as representing the official views or policies of the Department of Defense or the U.S. Government.

**Funding:** Listed authors from GE Research, Feinstein Institutes for Medical Research and North Shore University Hospital have received research funding from GE to investigate the effects of splenic ultrasound stimulation in healthy subjects. Listed authors from the University of Minnesota received funding from DARPA ElectRx Program (N660011824018).

**Author Contributions:** For research associated with splenic ultrasound in healthy participants and in rodents: K.W., J.A., C.P., S.S.C., T.R.C., J.P., K.J.T., S.Z. contributed to study design and setup; V.C., J.G., C.D'A., D.N., J.P. performed data collection and analysis; and C.P., V.C., T.C. contributed to data interpretation and writing. For research associated with splenic ultrasound of rheumatoid arthritis patients: R.S.G., D.P.Z., C.R.W.K., B.A.B., E.P., H.H.L. contributed to study design and setup; R.S.G., D.P.Z., C.R.W.K., E.P. performed data collection and analysis; R.S.G. performed data collection and bioinformatic analysis of single cell transcriptomic data; and R.S.G., D.P.Z., B.A.B., E.P., H.H.L contributed to data interpretation and writing. R.S.G., H.H.L. contributed to the first draft of the manuscript. All authors contributed to and approved the final version of the manuscript.

**Competing interests:** K.W., J.G., J.A., V.C., C.P. are employees of GE and declare that GE has filed U.S. and international patent applications describing methods, devices, and systems for precision organ-based ultrasound neuromodulation. R.S.G., D.P.Z., C.R.W.K., H.H.L are affiliated with University of Minnesota and declare that they have filed U.S. and international patent applications describing methods, devices, and systems for peripheral nerve and end-organ modulation. Feinstein authors have received research funding from GE to investigate the effects of splenic ultrasound in healthy subjects. Dr. Hubert Lim holds equity in, and serves as Chief Scientific Officer of, SecondWave Systems, which is developing wearable ultrasound stimulation technologies for end-organ and neural modulation. Mr. Daniel Zachs holds equity in, and is an employee of, SecondWave Systems. These interests for Dr. Lim and Mr. Zachs have been reviewed and managed by the University of Minnesota in accordance with its Conflict of Interest policies. All other authors declare that they have no competing interests.

**Data and Materials availability:**

Data associated with this study are presented in this paper or supplemental document. The RNA-seq data presented in this paper have been deposited in the Gene Expression Omnibus database as GSExxxxxx. Other data or methods such as that used for bioinformatic analyses or visualization are available upon reasonable request.

**Supplementary**

Figure S1. Modulation of Cytokines with Splenic Ultrasound in Rats
Figure S2. Cellular Transcriptional Signatures
Table S1. Single Cell RNA-seq: Number of Cells, Reads, and Genes
Table S2. Splenic Ultrasound in RA Patients: Subject Features
Table S3. Top 40 Enriched GO Terms for Downregulated Genes in Monocytes
Table S4. Cell Type Counts Per Participant and Statistics
Table S5. Splenic Ultrasound in Healthy Participants: Subject Features

Fig. S1

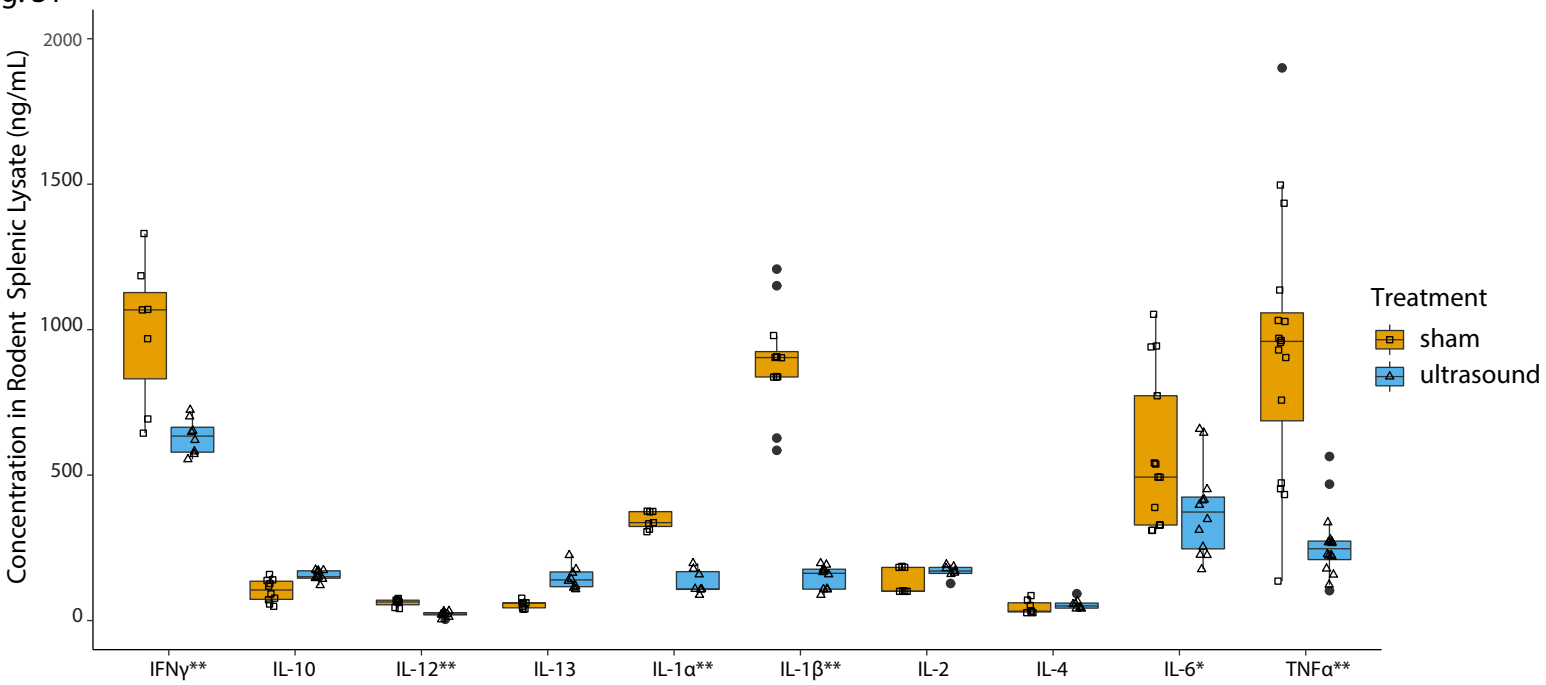


Figure S1. Modulation of Cytokines with Splenic Ultrasound in Rats. Splenic ultrasound was applied to rats for 2 minutes, daily for 3 days prior to the day of intraperitoneal LPS injection. Boxplot shows cytokine levels in splenic lysates from animals 1 hour post LPS injection receiving ultrasound or sham stimulation. Sham treated animals are shown with orange boxes with open squares representing individual data points, ultrasound stimulated animals shown with blue boxes and open triangles representing individual datapoints, solid black dots represent outliers. Cytokines that show a significant reduction with ultrasound are labeled with one asterisk based on a one-sided unpaired Wilcoxon rank-sum test ($p<0.05$; expecting a reduction in cytokines). Cytokines with two asterisks correspond to a $p<0.005$. Significant reduction is observed in IFNγ, IL-12, IL-1α, IL-1β, IL-6, TNF.

| Cytokine | # sham samples | # stim samples | one-sided unpaired Wilcoxon rank sum p-value |
|---|---|---|---|
| IFNγ | 7 | 8 | 0.004662 |
| IL-10 | 10 | 9 | 0.999500 |
| IL-12 | 7 | 9 | 0.000508 |
| IL-13 | 7 | 8 | 1.000000 |
| IL-1α | 7 | 7 | 0.000291 |
| IL-1β | 11 | 9 | 0.000002 |
| IL-2 | 7 | 7 | 0.875200 |
| IL-4 | 7 | 8 | 0.884100 |
| IL-6 | 12 | 12 | 0.034160 |
| TNF | 18 | 16 | 0.000001 |

Fig. S2

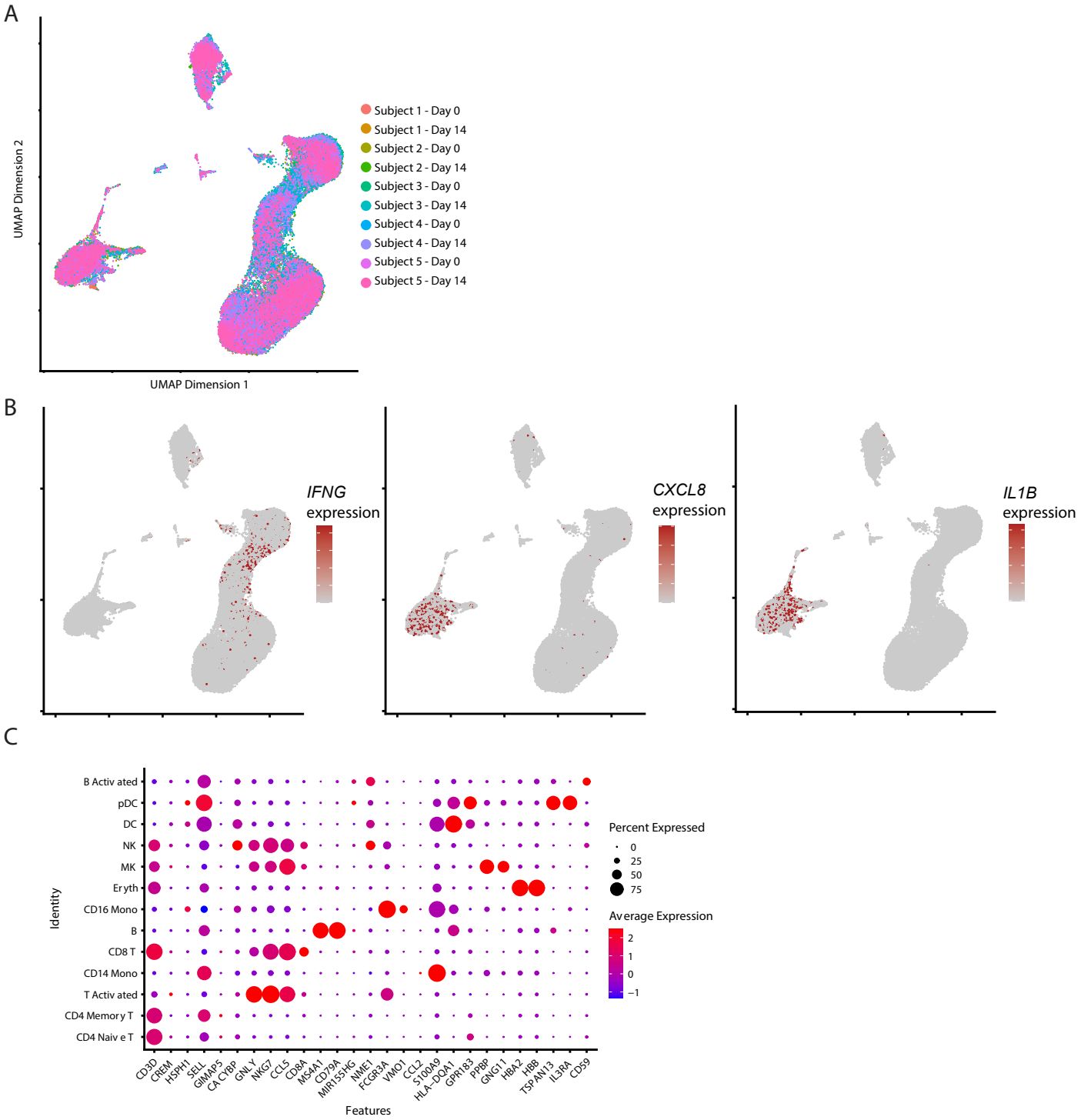


Figure S2. Cellular Transcriptional Signatures. Single cell RNA sequencing results on peripheral blood mononuclear cells. Uniform Manifold Approximation and Projection (UMAP) dimensionality reduction was used on principal component analysis which determines which gene sets contribute the most variability among the dataset.
A. UMAP plot of cells from each subject and timepoint to show transcriptional similarities between subjects and timepoints. B. UMAP plot shows cells expressing IFNG, CXCL8 and IL1B transcripts, and their expression patterns within particular cell types match with which cell types show statistical differential expression for those transcripts.
C. Dotplot showing the expression (color) and percent of cells expressing (dot size) each gene transcript (x-axis) for each cell type (y-axis). The genes listed on the x-axis are commonly used marker genes which help determine and assign cell types to groups of cells from an unbiased principal component analysis.

Table S1

| celltype | # of cells | total counts | average counts/cell | average genes/cell |
|---|---|---|---|---|
| B Activated day 0 | 20 | 1.57E+05 | 7.85E+03 | 2171 |
| B Activated day 14 | 24 | 1.53E+05 | 6.38E+03 | 1815 |
| B day 0 | 2485 | 8.87E+06 | 3.57E+03 | 1134 |
| B day 14 | 1835 | 6.88E+06 | 3.75E+03 | 1151 |
| CD14 Mono day 0 | 3465 | 1.69E+07 | 4.87E+03 | 1878 |
| CD14 Mono day 14 | 2150 | 9.77E+06 | 4.54E+03 | 1743 |
| CD16 Mono day 0 | 434 | 2.77E+06 | 6.37E+03 | 2184 |
| CD16 Mono day 14 | 324 | 1.97E+06 | 6.08E+03 | 2073 |
| CD4 Memory T day 0 | 8568 | 2.60E+07 | 3.03E+03 | 955 |
| CD4 Memory T day 14 | 4063 | 1.16E+07 | 2.86E+03 | 914 |
| CD4 Naive T day 0 | 7206 | 2.55E+07 | 3.55E+03 | 1154 |
| CD4 Naive T day 14 | 3629 | 1.17E+07 | 3.21E+03 | 1080 |
| CD8 T day 0 | 5764 | 1.63E+07 | 2.83E+03 | 1095 |
| CD8 T day 14 | 2505 | 7.78E+06 | 3.11E+03 | 1178 |
| DC day 0 | 138 | 1.19E+06 | 8.62E+03 | 2403 |
| DC day 14 | 102 | 8.41E+05 | 8.24E+03 | 2365 |
| Eryth day 0 | 388 | 1.19E+06 | 3.06E+03 | 875 |
| Eryth day 14 | 356 | 1.34E+06 | 3.77E+03 | 993 |
| MK day 0 | 288 | 7.48E+05 | 2.60E+03 | 1027 |
| MK day 14 | 130 | 3.40E+05 | 2.62E+03 | 1063 |
| NK day 0 | 78 | 4.30E+05 | 5.51E+03 | 1956 |
| NK day 14 | 192 | 1.14E+06 | 5.93E+03 | 1991 |
| pDC day 0 | 49 | 2.85E+05 | 5.82E+03 | 2080 |
| pDC day 14 | 74 | 3.94E+05 | 5.32E+03 | 1921 |
| T Activated day 0 | 5545 | 1.46E+07 | 2.63E+03 | 1162 |
| T Activated day 14 | 3531 | 9.02E+06 | 2.55E+03 | 1144 |
| **Total** | **53343** | **1.78E+08** | | |

Table S1. Single Cell RNA-seq: Number of Cells, Reads, and Genes. Table showing the number of cells for each cell type, which were determined by gene signatures (see Fig. S2C), and also showing number of reads (counts) and average number of genes for each cell type. We observe that all that all cells have a relatively consistent read depth for the sequencing reaction performed.

Table S2

| **Medical History and RA Features** (at time of first visit) | **Participant A** | **Participant B** | **Participant C** | **Participant D** | **Participant E** |
|---|---|---|---|---|---|
| Visit 1 Date | 4/18/2019 | 5/23/2019 | 8/29/2019 | 12/2/2019 | 12/2/2019 |
| Age | 68 | 57 | 89 | 42 | 41 |
| Sex | Female | Female | Male | Female | Female |
| Ethnic Group (as indicated in medical records) | American | American | American | Hmong | "Patient chose not to answer" |
| Height (inches) | 60 | 65 | 67 | 56 | 65 |
| Weight (lbs) | 180 | 139 | 170 | 118 | 256 |
| Body Mass Index | 35.2 | 23.1 | 26.6 | 26.5 | 43.3 |
| Date of RA diagnosis | 3/4/2019 | 6/1/2014 | 8/20/2019 | 1/1/2013 | 12/6/2013 |
| Time since RA diagnosis | 1 month | 4 years | 1 week | 6 years | 5 years |
| Prescription medicine for RA immune modulation which participants continued taking during study | Prednisone | None | None | Hydroxychloroquine | Orencia, methotrexate |
| Prescription medicine for pain taken during study | None | Hydrocodone | None | None | None |
| Non-prescription pain medicine taken during study | Acetaminophen | None | Ibuprofen, Aspirin | Acetaminophen, Naproxen | Naproxen |

Table S2. Splenic Ultrasound in RA Patients: Subject Features. Table showing key information for each participant, including age, sex, race, and medications the participants continued taking during the study. For figures in this publication where gene expression averages are shown per participant, participants are also shown as columns corresponding to A to E in this table.

Table S3

| | GO.ID | Term | Annotated | Significant | Expected | Rank in classicFisher | classicFisher | classicKS | elimKS | direction | sig_exp |
|---|---|---|---|---|---|---|---|---|---|---|---|
| 1 | GO:0043312 | neutrophil degranulation | 452 | 77 | 24.48 | 1 | 8.00E-19 | 0.958 | 0.958 | down | 3.145425 |
| 2 | GO:0000381 | regulation of alternative mRNA splicing,... | 58 | 17 | 3.14 | 2 | 6.00E-09 | 0.847 | 0.847 | down | 5.414013 |
| 3 | GO:2001243 | negative regulation of intrinsic apoptot... | 87 | 20 | 4.71 | 3 | 2.80E-08 | 0.768 | 0.768 | down | 4.246285 |
| 4 | GO:0030183 | B cell differentiation | 107 | 24 | 5.8 | 4 | 5.30E-08 | 0.986 | 0.986 | down | 4.137931 |
| 5 | GO:0045727 | positive regulation of translation | 116 | 22 | 6.28 | 5 | 2.20E-07 | 0.817 | 0.817 | down | 3.503185 |
| 6 | GO:0016032 | viral process | 783 | 80 | 42.41 | 6 | 8.30E-07 | 0.497 | 0.497 | down | 1.886348 |
| 7 | GO:0000122 | negative regulation of transcription by ... | 693 | 68 | 37.54 | 7 | 1.20E-06 | 0.982 | 0.982 | down | 1.811401 |
| 8 | GO:0017148 | negative regulation of translation | 124 | 26 | 6.72 | 8 | 2.10E-06 | 0.747 | 0.747 | down | 3.869048 |
| 9 | GO:0045944 | positive regulation of transcription by ... | 947 | 87 | 51.3 | 9 | 2.70E-06 | 0.864 | 0.864 | down | 1.695906 |
| 10 | GO:0042535 | positive regulation of tumor necrosis fa... | 19 | 8 | 1.03 | 10 | 3.20E-06 | 0.929 | 0.929 | down | 7.76699 |
| 11 | GO:0045410 | positive regulation of interleukin-6 bio... | 15 | 7 | 0.81 | 11 | 5.80E-06 | 0.93 | 0.93 | down | 8.641975 |
| 12 | GO:0006954 | inflammatory response | 575 | 68 | 31.15 | 12 | 1.50E-05 | 0.146 | 0.146 | down | 2.182986 |
| 13 | GO:1903204 | negative regulation of oxidative stress-... | 18 | 7 | 0.98 | 13 | 2.50E-05 | 0.553 | 0.553 | down | 7.142857 |
| 14 | GO:0090316 | positive regulation of intracellular pro... | 166 | 26 | 8.99 | 14 | 3.20E-05 | 0.788 | 0.788 | down | 2.892102 |
| 15 | GO:0045766 | positive regulation of angiogenesis | 134 | 20 | 7.26 | 15 | 3.40E-05 | 1 | 1 | down | 2.754821 |
| 16 | GO:0001774 | microglial cell activation | 39 | 12 | 2.11 | 16 | 4.50E-05 | 0.972 | 0.972 | down | 5.687204 |
| 17 | GO:0019221 | cytokine-mediated signaling pathway | 678 | 75 | 36.73 | 17 | 5.10E-05 | 0.351 | 0.927 | down | 2.041928 |
| 18 | GO:0071345 | cellular response to cytokine stimulus | 953 | 114 | 51.62 | 18 | 7.00E-05 | 0.127 | 0.492 | down | 2.208446 |
| 19 | GO:0045429 | positive regulation of nitric oxide bios... | 35 | 9 | 1.9 | 19 | 7.60E-05 | 0.97 | 0.97 | down | 4.736842 |
| 20 | GO:0002755 | MyD88-dependent toll-like receptor signa... | 35 | 9 | 1.9 | 20 | 7.60E-05 | 0.497 | 0.497 | down | 4.736842 |
| 21 | GO:1902532 | negative regulation of intracellular sig... | 442 | 61 | 23.94 | 21 | 7.70E-05 | 0.832 | 0.832 | down | 2.548037 |
| 22 | GO:0045416 | positive regulation of interleukin-8 bio... | 10 | 5 | 0.54 | 22 | 9.20E-05 | 0.924 | 0.924 | down | 9.259259 |
| 23 | GO:0043488 | regulation of mRNA stability | 166 | 31 | 8.99 | 23 | 9.30E-05 | 0.486 | 0.486 | down | 3.448276 |
| 24 | GO:0031663 | lipopolysaccharide-mediated signaling pa... | 53 | 11 | 2.87 | 24 | 0.0001 | 0.987 | 0.987 | down | 3.832753 |
| 25 | GO:0010803 | regulation of tumor necrosis factor-medi... | 53 | 11 | 2.87 | 25 | 0.0001 | 1 | 1 | down | 3.832753 |
| 26 | GO:0006915 | apoptotic process | 1625 | 171 | 88.02 | 26 | 0.0001 | 0.811 | 0.811 | down | 1.94274 |
| 27 | GO:0008360 | regulation of cell shape | 134 | 19 | 7.26 | 27 | 0.00011 | 0.731 | 0.731 | down | 2.61708 |
| 28 | GO:0035666 | TRIF-dependent toll-like receptor signal... | 29 | 8 | 1.57 | 28 | 0.00011 | 0.982 | 0.982 | down | 5.095541 |
| 29 | GO:0071260 | cellular response to mechanical stimulus | 72 | 13 | 3.9 | 29 | 0.00011 | 0.859 | 0.859 | down | 3.333333 |
| 30 | GO:0048255 | mRNA stabilization | 37 | 9 | 2 | 30 | 0.00012 | 0.085 | 0.085 | down | 4.5 |
| 31 | GO:0039535 | regulation of RIG-I signaling pathway | 16 | 6 | 0.87 | 31 | 0.00012 | 0.934 | 0.934 | down | 6.896552 |
| 32 | GO:0035690 | cellular response to drug | 336 | 38 | 18.2 | 32 | 0.00013 | 0.944 | 0.944 | down | 2.087912 |
| 33 | GO:0045588 | positive regulation of gamma-delta T cel... | 3 | 3 | 0.16 | 33 | 0.00016 | 0.998 | 0.998 | down | 18.75 |
| 34 | GO:0000186 | activation of MAPKK activity | 47 | 10 | 2.55 | 34 | 0.00017 | 0.998 | 0.998 | down | 3.921569 |
| 35 | GO:0032922 | circadian regulation of gene expression | 56 | 11 | 3.03 | 35 | 0.00017 | 0.861 | 0.861 | down | 3.630363 |
| 36 | GO:2001235 | positive regulation of apoptotic signali... | 162 | 21 | 8.78 | 36 | 0.00018 | 0.52 | 0.52 | down | 2.3918 |
| 37 | GO:0046777 | protein autophosphorylation | 210 | 25 | 11.38 | 37 | 0.00018 | 0.68 | 0.68 | down | 2.196837 |
| 38 | GO:0002902 | regulation of B cell apoptotic process | 17 | 6 | 0.92 | 38 | 0.00018 | 0.51 | 0.51 | down | 6.521739 |
| 39 | GO:0071456 | cellular response to hypoxia | 181 | 25 | 9.8 | 39 | 0.00019 | 0.909 | 0.909 | down | 2.55102 |
| 40 | GO:0030890 | positive regulation of B cell proliferat... | 39 | 9 | 2.11 | 40 | 0.00019 | 0.859 | 0.859 | down | 4.265403 |

Table S3. Top 40 Enriched GO Terms for Downregulated Genes in Monocytes. Table displaying enriched GO terms for genes downregulated with ultrasound treatment. Also shown are the number of genes out of the human genome that are annotated with that GO term, number of genes from the list of significantly downregulated genes with ultrasound, and the number of genes that would be expected by random chance. Column labeled 'classicFisher' shows p-values from the Fisher's exact test and 'sig_exp' is the number of genes found to be significant in our gene list (decreased with ultrasound in monocytes) compared to the number that might be expected by chance.

Table S4

| Participant | Timepoint | Cell Type | # of Cells Sequenced | paired Wilcoxon p-value comparing # of cells sequenced | Total # Cells Sequenced in Sample | Percent | paired Wilcoxon p-value comparing % of cells |
|---|---|---|---|---|---|---|---|
| A. | Day 0 | B | 182 | | 4074 | 4.467 | |
| B. | Day 0 | B | 6 | | 5501 | 0.109 | |
| C. | Day 0 | B | 639 | | 10930 | 5.846 | |
| D. | Day 0 | B | 790 | | 8527 | 9.265 | |
| E. | Day 0 | B | 868 | | 5396 | 16.086 | |
| A. | Day 14 | B | 12 | | 278 | 4.317 | |
| B. | Day 14 | B | 43 | | 3021 | 1.423 | |
| C. | Day 14 | B | 251 | | 4634 | 5.416 | |
| D. | Day 14 | B | 568 | | 5605 | 10.134 | |
| E. | Day 14 | B | 961 | 0.3125 | 5377 | 17.872 | 0.3125 |
| A. | Day 0 | B Activated | 1 | | 4074 | 0.025 | |
| B. | Day 0 | B Activated | 3 | | 5501 | 0.055 | |
| C. | Day 0 | B Activated | 7 | | 10930 | 0.064 | |
| D. | Day 0 | B Activated | 3 | | 8527 | 0.035 | |
| E. | Day 0 | B Activated | 6 | | 5396 | 0.111 | |
| B. | Day 14 | B Activated | 2 | | 3021 | 0.066 | |
| C. | Day 14 | B Activated | 10 | | 4634 | 0.216 | |
| D. | Day 14 | B Activated | 4 | | 5605 | 0.071 | |
| E. | Day 14 | B Activated | 8 | 0.3893 | 5377 | 0.149 | 0.06349 |
| A. | Day 0 | CD14 Mono | 758 | | 4074 | 18.606 | |
| B. | Day 0 | CD14 Mono | 507 | | 5501 | 9.217 | |
| C. | Day 0 | CD14 Mono | 879 | | 10930 | 8.042 | |
| D. | Day 0 | CD14 Mono | 471 | | 8527 | 5.524 | |
| E. | Day 0 | CD14 Mono | 850 | | 5396 | 15.752 | |
| A. | Day 14 | CD14 Mono | 124 | | 278 | 44.604 | |
| B. | Day 14 | CD14 Mono | 229 | | 3021 | 7.58 | |
| C. | Day 14 | CD14 Mono | 397 | | 4634 | 8.567 | |
| D. | Day 14 | CD14 Mono | 549 | | 5605 | 9.795 | |
| E. | Day 14 | CD14 Mono | 851 | 0.3125 | 5377 | 15.827 | 0.3125 |
| A. | Day 0 | CD16 Mono | 61 | | 4074 | 1.497 | |
| B. | Day 0 | CD16 Mono | 129 | | 5501 | 2.345 | |
| C. | Day 0 | CD16 Mono | 159 | | 10930 | 1.455 | |
| D. | Day 0 | CD16 Mono | 53 | | 8527 | 0.622 | |
| E. | Day 0 | CD16 Mono | 32 | | 5396 | 0.593 | |
| A. | Day 14 | CD16 Mono | 12 | | 278 | 4.317 | |
| B. | Day 14 | CD16 Mono | 58 | | 3021 | 1.92 | |
| C. | Day 14 | CD16 Mono | 165 | | 4634 | 3.561 | |
| D. | Day 14 | CD16 Mono | 25 | | 5605 | 0.446 | |
| E. | Day 14 | CD16 Mono | 64 | 0.4375 | 5377 | 1.19 | 0.3125 |
| A. | Day 0 | CD4 Memor | 1087 | | 4074 | 26.681 | |
| B. | Day 0 | CD4 Memor | 1814 | | 5501 | 32.976 | |
| C. | Day 0 | CD4 Memor | 1865 | | 10930 | 17.063 | |
| D. | Day 0 | CD4 Memor | 2808 | | 8527 | 32.931 | |
| E. | Day 0 | CD4 Memor | 994 | | 5396 | 18.421 | |
| A. | Day 14 | CD4 Memor | 45 | | 278 | 16.187 | |
| B. | Day 14 | CD4 Memor | 915 | | 3021 | 30.288 | |
| C. | Day 14 | CD4 Memor | 778 | | 4634 | 16.789 | |
| D. | Day 14 | CD4 Memor | 1422 | | 5605 | 25.37 | |
| E. | Day 14 | CD4 Memor | 903 | 0.0625 | 5377 | 16.794 | 0.0625 |
| A. | Day 0 | CD4 Naive T | 1245 | | 4074 | 30.56 | |
| B. | Day 0 | CD4 Naive T | 1260 | | 5501 | 22.905 | |
| C. | Day 0 | CD4 Naive T | 1686 | | 10930 | 15.425 | |
| D. | Day 0 | CD4 Naive T | 1788 | | 8527 | 20.969 | |
| E. | Day 0 | CD4 Naive T | 1227 | | 5396 | 22.739 | |
| A. | Day 14 | CD4 Naive T | 48 | | 278 | 17.266 | |
| B. | Day 14 | CD4 Naive T | 609 | | 3021 | 20.159 | |
| C. | Day 14 | CD4 Naive T | 887 | | 4634 | 19.141 | |
| D. | Day 14 | CD4 Naive T | 842 | | 5605 | 15.022 | |
| E. | Day 14 | CD4 Naive T | 1243 | 0.125 | 5377 | 23.117 | 0.4375 |
| A. | Day 0 | CD8 T | 459 | | 4074 | 11.267 | |
| B. | Day 0 | CD8 T | 542 | | 5501 | 9.853 | |
| C. | Day 0 | CD8 T | 3107 | | 10930 | 28.426 | |
| D. | Day 0 | CD8 T | 1193 | | 8527 | 13.991 | |
| E. | Day 0 | CD8 T | 463 | | 5396 | 8.58 | |

| Participant | Timepoint | Cell Type | # of Cells | | paired Wilcoxon p-value comparing # of cells sequenced | Percent | paired Wilcoxon p-value comparing % of cells |
|---|---|---|---|---|---|---|---|
| A. | Day 14 | CD8 T | 15 | | 278 | 5.396 | |
| B. | Day 14 | CD8 T | 287 | | 3021 | 9.5 | |
| C. | Day 14 | CD8 T | 967 | | 4634 | 20.868 | |
| D. | Day 14 | CD8 T | 846 | | 5605 | 15.094 | |
| E. | Day 14 | CD8 T | 390 | 0.0625 | 5377 | 7.253 | 0.1875 |
| A. | Day 0 | DC | 15 | | 4074 | 0.368 | |
| B. | Day 0 | DC | 45 | | 5501 | 0.818 | |
| C. | Day 0 | DC | 19 | | 10930 | 0.174 | |
| D. | Day 0 | DC | 15 | | 8527 | 0.176 | |
| E. | Day 0 | DC | 44 | | 5396 | 0.815 | |
| A. | Day 14 | DC | 3 | | 278 | 1.079 | |
| B. | Day 14 | DC | 15 | | 3021 | 0.497 | |
| C. | Day 14 | DC | 11 | | 4634 | 0.237 | |
| D. | Day 14 | DC | 12 | | 5605 | 0.214 | |
| E. | Day 14 | DC | 61 | 0.4375 | 5377 | 1.134 | 0.4375 |
| A. | Day 0 | Eryth | 8 | | 4074 | 0.196 | |
| B. | Day 0 | Eryth | 3 | | 5501 | 0.055 | |
| C. | Day 0 | Eryth | 12 | | 10930 | 0.11 | |
| D. | Day 0 | Eryth | 238 | | 8527 | 2.791 | |
| E. | Day 0 | Eryth | 127 | | 5396 | 2.354 | |
| A. | Day 14 | Eryth | 1 | | 278 | 0.36 | |
| B. | Day 14 | Eryth | 3 | | 3021 | 0.099 | |
| C. | Day 14 | Eryth | 15 | | 4634 | 0.324 | |
| D. | Day 14 | Eryth | 261 | | 5605 | 4.657 | |
| E. | Day 14 | Eryth | 76 | 0.8551 | 5377 | 1.413 | 0.4375 |
| A. | Day 0 | MK | 34 | | 4074 | 0.835 | |
| B. | Day 0 | MK | 5 | | 5501 | 0.091 | |
| C. | Day 0 | MK | 129 | | 10930 | 1.18 | |
| D. | Day 0 | MK | 95 | | 8527 | 1.114 | |
| E. | Day 0 | MK | 25 | | 5396 | 0.463 | |
| A. | Day 14 | MK | 1 | | 278 | 0.36 | |
| B. | Day 14 | MK | 11 | | 3021 | 0.364 | |
| C. | Day 14 | MK | 50 | | 4634 | 1.079 | |
| D. | Day 14 | MK | 59 | | 5605 | 1.053 | |
| E. | Day 14 | MK | 9 | 0.125 | 5377 | 0.167 | 0.3125 |
| A. | Day 0 | NK | 16 | | 4074 | 0.393 | |
| B. | Day 0 | NK | 18 | | 5501 | 0.327 | |
| C. | Day 0 | NK | 18 | | 10930 | 0.165 | |
| D. | Day 0 | NK | 16 | | 8527 | 0.188 | |
| E. | Day 0 | NK | 10 | | 5396 | 0.185 | |
| A. | Day 14 | NK | 1 | | 278 | 0.36 | |
| B. | Day 14 | NK | 20 | | 3021 | 0.662 | |
| C. | Day 14 | NK | 126 | | 4634 | 2.719 | |
| D. | Day 14 | NK | 31 | | 5605 | 0.553 | |
| E. | Day 14 | NK | 14 | 0.343 | 5377 | 0.26 | 0.125 |
| A. | Day 0 | pDC | 2 | | 4074 | 0.049 | |
| B. | Day 0 | pDC | 14 | | 5501 | 0.254 | |
| C. | Day 0 | pDC | 7 | | 10930 | 0.064 | |
| D. | Day 0 | pDC | 6 | | 8527 | 0.07 | |
| E. | Day 0 | pDC | 20 | | 5396 | 0.371 | |
| A. | Day 14 | pDC | 3 | | 278 | 1.079 | |
| B. | Day 14 | pDC | 29 | | 3021 | 0.96 | |
| C. | Day 14 | pDC | 9 | | 4634 | 0.194 | |
| D. | Day 14 | pDC | 12 | | 5605 | 0.214 | |
| E. | Day 14 | pDC | 21 | 0.05791 | 5377 | 0.391 | 0.0625 |
| A. | Day 0 | T Activated | 206 | | 4074 | 5.056 | |
| B. | Day 0 | T Activated | 1155 | | 5501 | 20.996 | |
| C. | Day 0 | T Activated | 2403 | | 10930 | 21.985 | |
| D. | Day 0 | T Activated | 1051 | | 8527 | 12.326 | |
| E. | Day 0 | T Activated | 730 | | 5396 | 13.529 | |
| A. | Day 14 | T Activated | 13 | | 278 | 4.676 | |
| B. | Day 14 | T Activated | 800 | | 3021 | 26.481 | |
| C. | Day 14 | T Activated | 968 | | 4634 | 20.889 | |
| D. | Day 14 | T Activated | 974 | | 5605 | 17.377 | |
| E. | Day 14 | T Activated | 776 | 0.125 | 5377 | 14.432 | 0.4375 |

Table S4. Cell Type Counts Per Participant and Statistics. Table displaying the number of cells sequenced and percent (# cells in cell type / # cells sequenced in that sample x 100) for each sample (defined as a participant and timepoint) per cell type. No significant difference is seen in the number of cell sequenced per cell type or percent within each cell type comparing pre- and post ultrasound stimulation with a paired Wilcoxon rank sum test that was used to determine p-values.

Table S5

| Subject | 1 | 2 | 3 | 4 | 5 | 6 | 7 | 8 | 9 | 10 |
|---|---|---|---|---|---|---|---|---|---|---|
| Group | Stimulated | Stimulated | Stimulated | Stimulated | Stimulated | Stimulated | Stimulated | Stimulated | Stimulated | Stimulated |
| Age | 35 | 39 | 29 | 39 | 44 | 30 | 28 | 35 | 32 | 42 |
| Gender | Female | Female | Male | Female | Female | Female | Male | Female | Female | Female |
| Race | Asian | Asian | More Than One Race | Other | Black or African American | More Than One Race | Other | Other | White or Caucasian | White or Caucasian |
| Ethnicity | Not Hispanic or Latino | Not Hispanic or Latino | Not Hispanic or Latino | Hispanic or Latino | Not Hispanic or Latino | Hispanic or Latino | Not Hispanic or Latino | Hispanic or Latino | Hispanic or Latino | Not Hispanic or Latino |
| Height (cm) | 177 | 165 | 188 | 159 | 164 | 168 | 195 | 160 | 156 | 168 |
| Weight (kg) | 64 | 58.5 | 94.6 | 69.8 | 64.5 | 67 | 79.1 | 55.8 | 58.7 | 70 |
| Body Mass Index (kg/m2) | 20.4 | 21.5 | 26.8 | 27.6 | 24 | 23.7 | 20.8 | 21.8 | 24.1 | 24.8 |
| Medicines & Supplements | | | Multi Vitamin | Multi Vitamin | Multi Vitamin | | | | | |
| Conditions | | | Hemo-phagocytic Lympho-histiocytosis 14 years ago | | | | | | Gestational diabetes in prior 3 years. Resolved after delivery. | Mitral Value Prolapse, Current - No treatment needed |
| Exclusion Reason | Excluded : incorrect imaging protocol applied | | | | | | | | | |

| Subject | 11 | 12 | 13 | 14 | 15 | 16 | 17 | 18 | 19 | 20 |
|---|---|---|---|---|---|---|---|---|---|---|
| Group | Control | Control | Control | Control | Control | Control | Control | Control | Control | Control |
| Age | 22 | 27 | 32 | 18 | 36 | 33 | 27 | 40 | 28 | 28 |
| Gender | Female | Male | Female | Male | Male | Female | Female | Male | Male | Male |
| Race | White or Caucasian | Asian | Black or African American | Asian | Asian | Asian | Asian | Asian | Asian | Other |
| Ethnicity | Not Hispanic or Latino | Not Hispanic or Latino | Not Hispanic or Latino | Not Hispanic or Latino | Not Hispanic or Latino | Not Hispanic or Latino | Not Hispanic or Latino | Not Hispanic or Latino | Not Hispanic or Latino | Hispanic or Latino |
| Height (cm) | 162 | 176 | 173 | 183 | 176 | 161 | 155 | 166 | 172.25 | 180 |
| Weight (kg) | 73.9 | 72 | 72.9 | 72.3 | 80.9 | 58.2 | 61.1 | 67 | 81.5 | 75.4 |
| Body Mass Index (kg/m2) | 28.2 | 23.2 | 24.4 | 21.6 | 26.1 | 22.5 | 25.4 | 24.3 | 27.5 | 23.3 |
| Medicines & Supplements | | Vitamin D, EOD 5000 IU, Promote Health | | | Multi Vitamin, Fish Oil | Multi Vitamin | | | Pantoperazole 20 mg daily, acid reflux | Multi Vitamin |
| Conditions | Acid Reflux | | | | Jaundice at 7 years of age, resolved | | | | | |
| Exclusion Reason | | | | | | | | | Excluded : glucose <50 mg/dL at baseline | |

Table S6. Splenic Ultrasound in Healthy Participants: Subject Features. Characteristics and demographic data of 20 enrolled subjects for study of biological effects of ultrasound of the spleen. Ten subjects received full-powered ultrasound treatment at the spleen hilum and another ten subjects were sham controls with the ultrasound device turned off. One of the subjects from the stimulated group was excluded due the selection of the wrong ultrasound imaging protocol by the clinician. One of the subjects from the control group was excluded because their baseline glucose measurement was <50 mg/dL that is considered hypoglycemic.